Gamma-ray astronomy and multi-messenger astrophysics

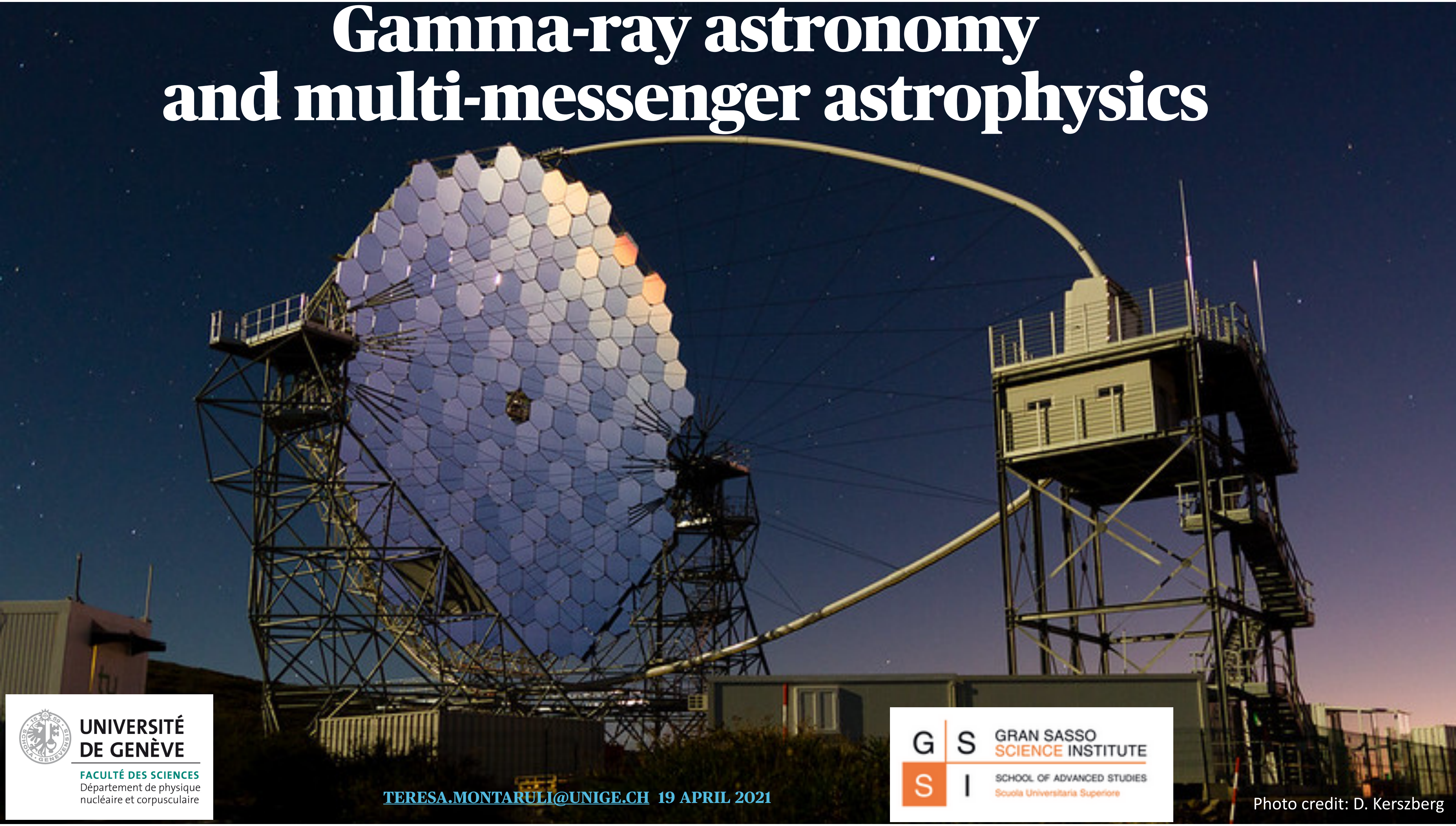

Photo credit: D. Kerszberg

UNIVERSITÉ DE GENÈVE
FACULTÉ DES SCIENCES
Département de physique nucléaire et corpusculaire

TERESA.MONTARULI@UNIGE.CH 19 APRIL 2021

GSSI GRAN SASSO SCIENCE INSTITUTE
SCHOOL OF ADVANCED STUDIES
Scuola Universitaria Superiore

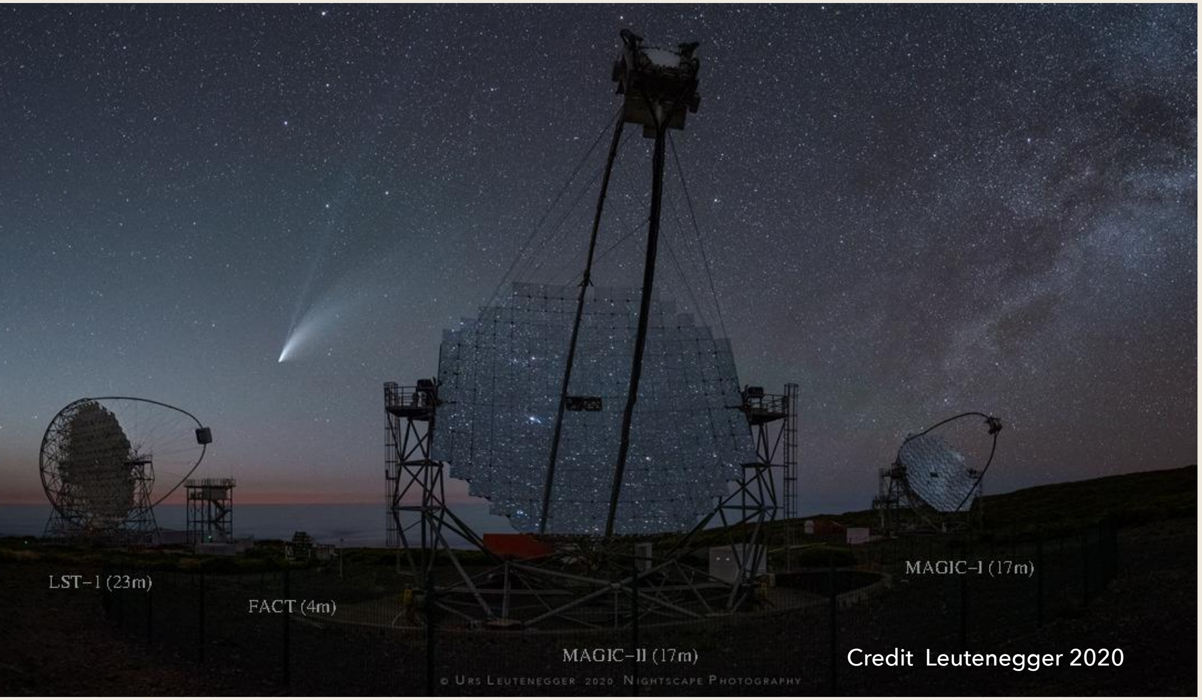

Contents

- Gamma-ray astronomy technique and science scopes
  - Cosmic ray sources
  - New Physics frontier

- Major experimental efforts in ground based gamma-ray astronomy:
  - CTA Observatory status and first results
  - The LHAASO and UHE gamma-rays

- Instrumentation and R&D towards future large size cameras

Gamma-ray in roadmaps for the future

- First recommendation in Astroparticle Physics European Consortium (APPEC) Roadmap 2017-2026 is on **CTAO timely construction & securing its long term operation**;
- ASTRONET Roadmap Community Consultation: not much on gamma-ray in its first stage…ASTRONET is mostly in charge of ground-based astronomy, and X and gamma-rays from space covered by ESA;

Neutrino GW Gamma-ray Astrophysics

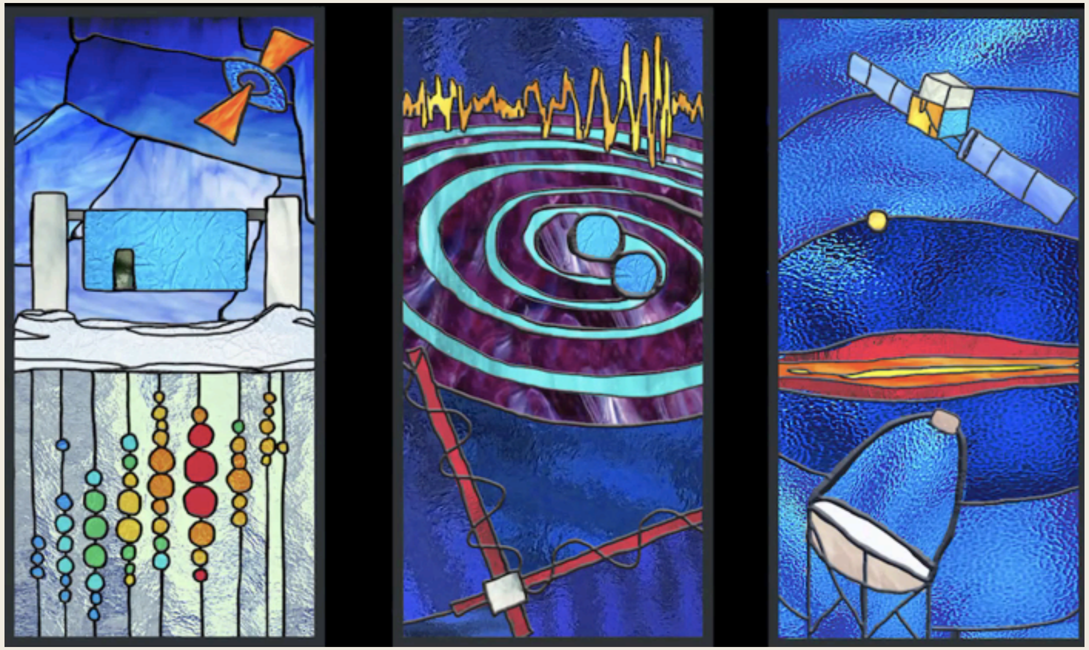

- Ground-based gamma-ray astronomy is a success story but mostly seen as a `particle acceleration' of interest for astroparticle physicists (APPEC)?
- Nonetheless, a new revolution is taking place: **multi-messenger astrophysics**, which encompasses frontiers… different communities, different instruments, different methodologies.
- This is a great challenge of exchange between particle physicists and astronomers, also recognised in the European Particle Physics Strategy Update (EPPSU 2018-2020) process recommendation:

B. Astroparticle physics, coordinated by APPEC in Europe, also addresses questions about the fundamental physics of particles and their interactions. The ground-breaking discovery of gravitational waves has occurred since the last Strategy update, and this has contributed to burgeoning multi-messenger observations of the universe. ***Synergies between particle and astroparticle physics should be strengthened through scientific exchanges and technological cooperation in areas of common interest and mutual benefit.***

Gamma-astronomy `themes'

https://arxiv.org/abs/1709.07997

- ***Understanding of the origin of the cosmic rays*** in a multi-messenger context ;
- ***Probing extreme environments,*** such as neutron stars, black holes and gamma-ray bursts, the physics of the jets and how particles are accelerated by them;
- ***The Galactic plane Survey*** (*deep survey 2 mCU, faster by ~100 than current generation)*;
- ***Exploring frontiers in physics***, such as the nature of Dark Matter in the Galactic Centre, axions and their interplay with magnetic fields and photons, the extragalactic background light and how it informs on galaxy formation, and quantum gravitational effects in photon propagation.

Gamma-ray astronomy sensitivity to source fluxes

eASTROGAM Science book De Angelis & Mallamaci, https://arxiv.org/abs/1805.05642

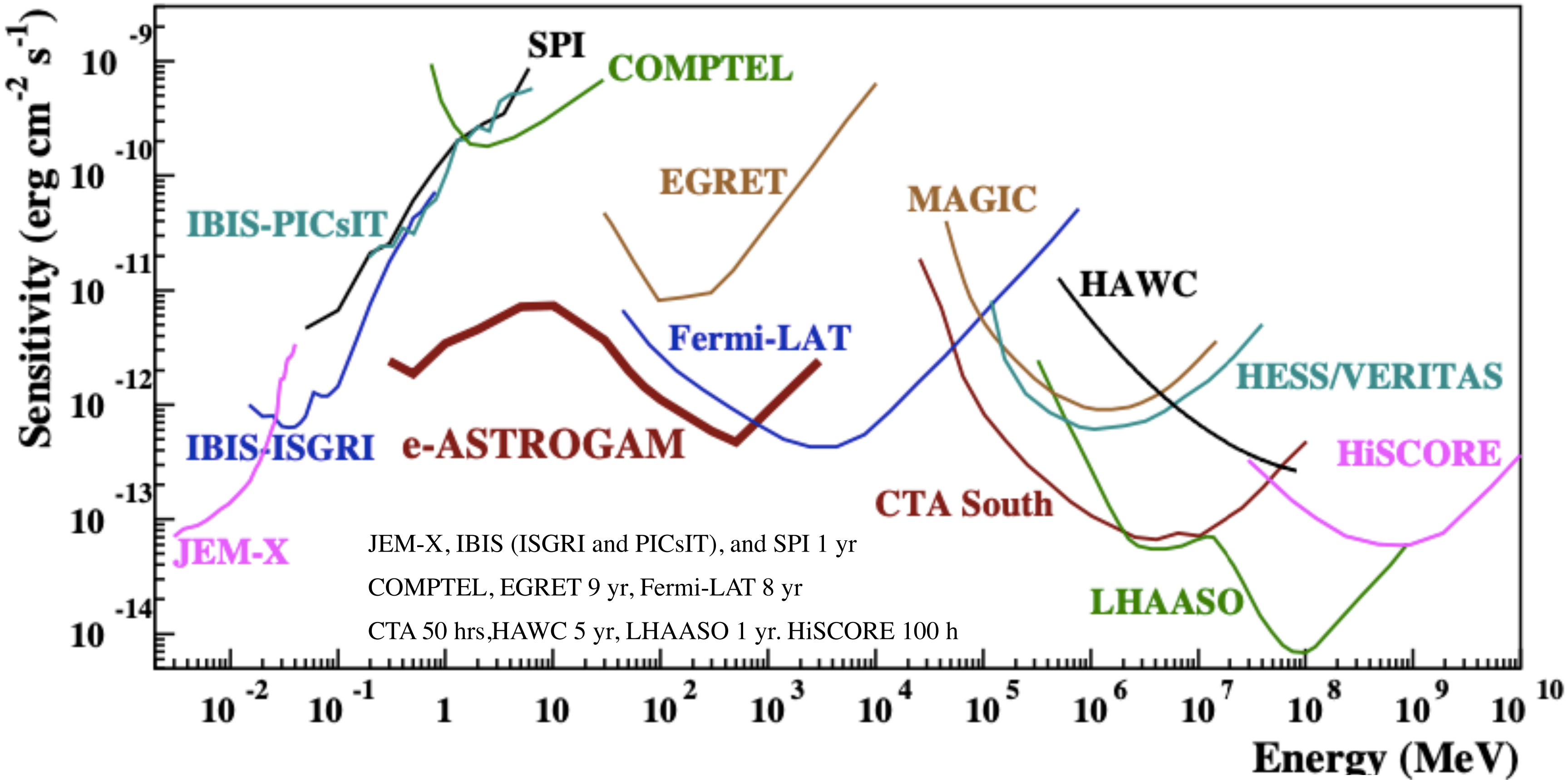

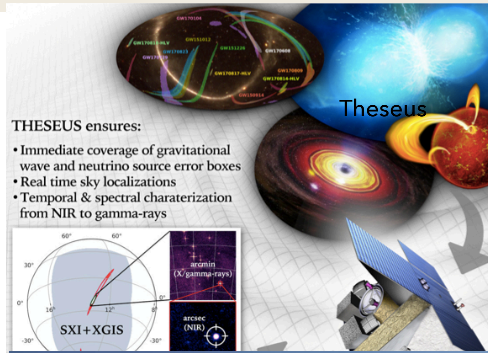

From space < 300 GeV up to 2035:

Fermi-LAT

Athena: X-ray mission approved for L2

Theseus for GRB&high energy transients, M5 selection in these days

>20 GeV - 1 TeV (IACT)

- Pulsars, GRBs, fast transients
- nearby blazars, Mkn 421, Mrk 501, radiogalaxy M87
  - Dark matter in the Galactic Centre and dwarf spheroidal galaxies dSphs

UHE > 100 TeV (IACT arrays, EAS)

Galactic PeVatrons:SNR molecular clouds, Pulsar Wind Nebulae)

Gamma-ray detection

From ground

Imaging Air Cherenkov Telescopes (IACT)

- atmosphere is calorimeter
- Sets of mirrors focus Cherenkov pool light into fast camera in focus
- ~10% duty cycle due to Moon and weather and exposed mirrors
- decreasing efficiency by order of 2% due to mirror deterioration

Quantity	*Fermi*	IACTs	EAS
Energy range	20 MeV – 200 GeV	100 GeV – 50 TeV	400 GeV – 100 TeV
Energy res.	5–10 %	15–20 %	$\sim$ 50 %
Duty cycle	80 %	15 %	$>$ 90 %
FoV	$4\pi/5$	5 deg $\times$ 5 deg	$4\pi/6$
PSF (deg)	0.1	0.07	0.5
Sensitivity	1 % Crab (1 GeV)	1 % Crab (0.5 TeV)	0.5 Crab (5 TeV)

Table from De Angelis, Mallamaci, arXiv:0805.05642

Space-based : 0.1 - 100 GeV
Large FoV and duty cycle

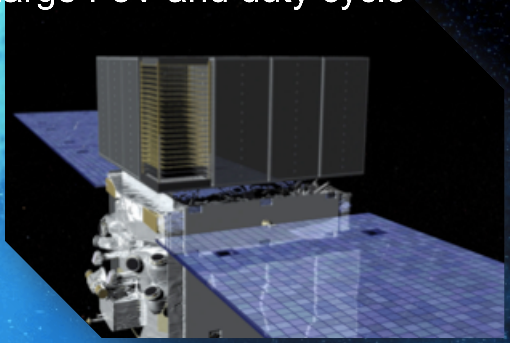

EAS: $\gtrsim$1 TeV

- collect Cherenkov radiation produced by charged particles in water tanks or ponds equipped with photosensors
- > 90% duty cycle and large FoV
- Needs water purification and recycling (HAWC, LHAASO)
- Future Southern Widefield Gamma-ray Observatory (SWGO)

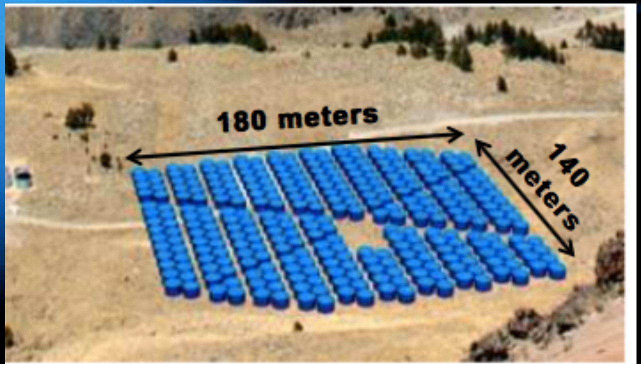

Imaging Air Cherenkov Telescopes

C. Galbreith & J. Jelley, when visiting the Harwell Air Shower Array in UK in 1952, used a a 5 cm PMT mounted on the focal plane of a 25 cm parabolic mirror in a garbage can. They observed oscilloscope triggers from light pulses that exceeded the average night-sky background every 2 min. In 1953, from the polarisation and spectral distribution, they confirmed P. Backett's assertion that Cherenkov light is produced by charged CRs in the atmosphere on top of the night sky background.

In 1959 G. Cocconi proposed to measure TeV gamma-rays using air shower detectors.

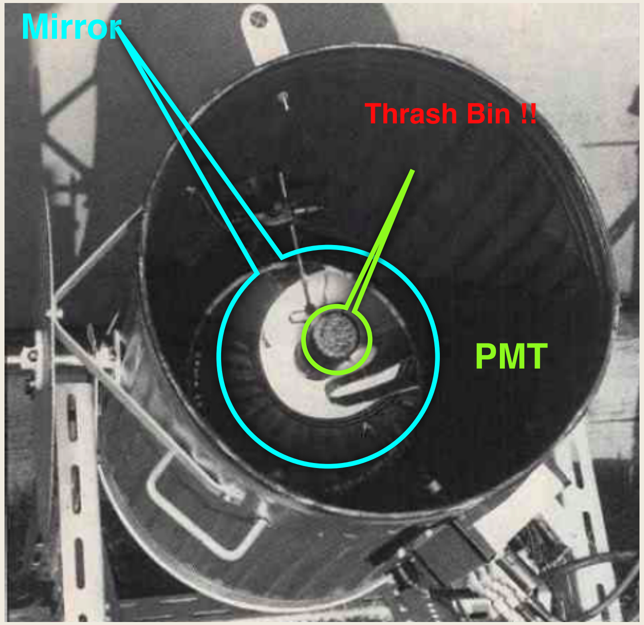

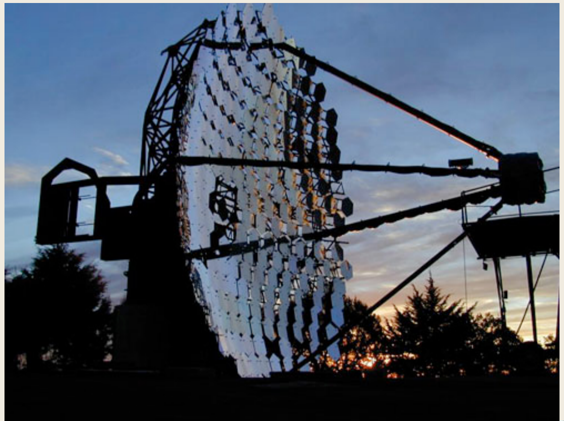

Trevor Weekes (1940-2014) Whipple,Crab Nebula discovery 1989

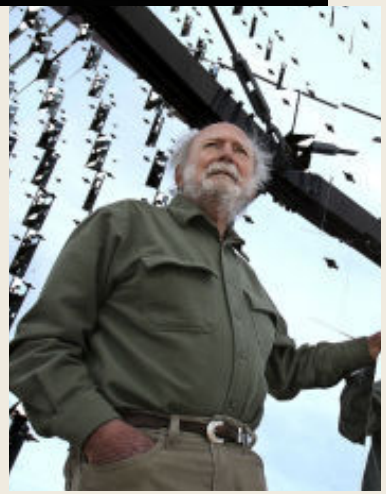

Eckart Lorenz (1938-2014) HEGRA+AIROBICC, MAGIC arrays

Imaging Cherenkov technology

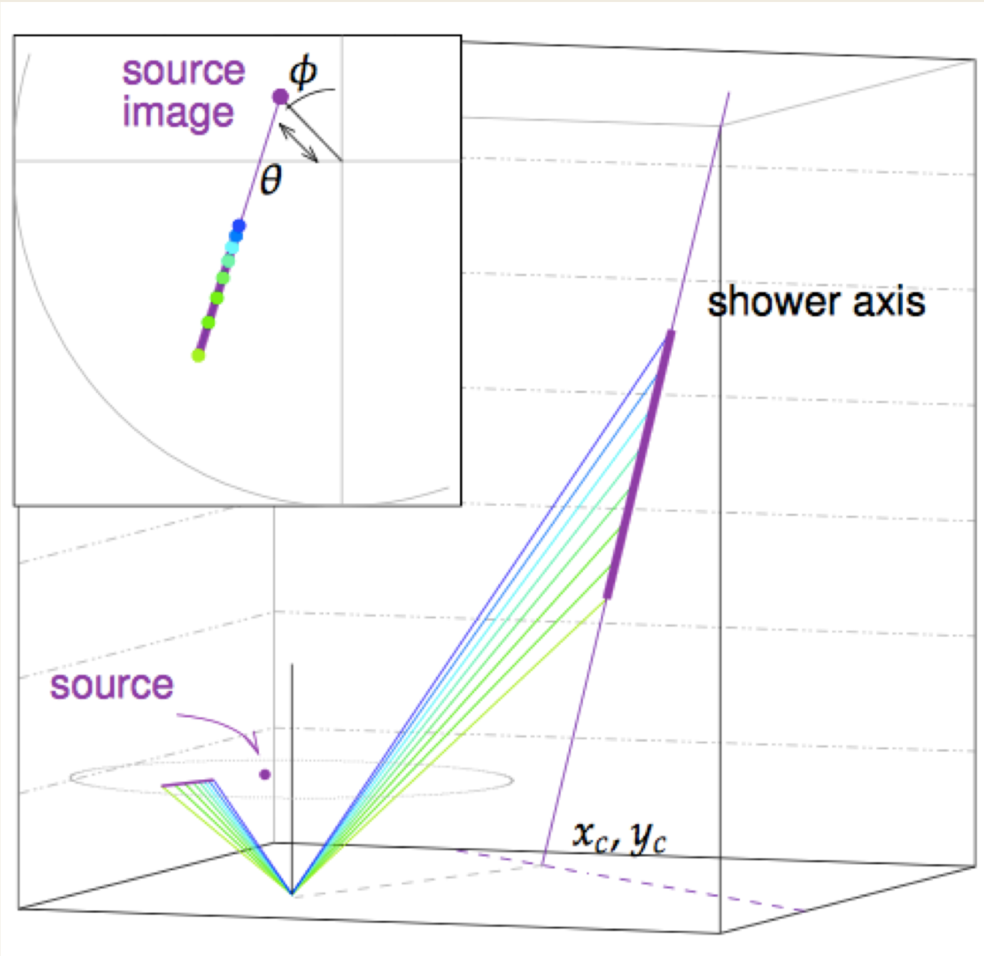

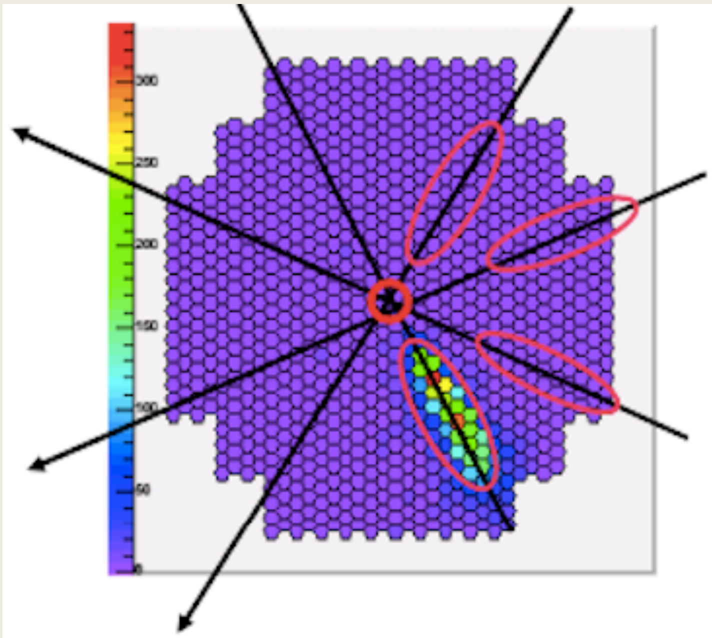

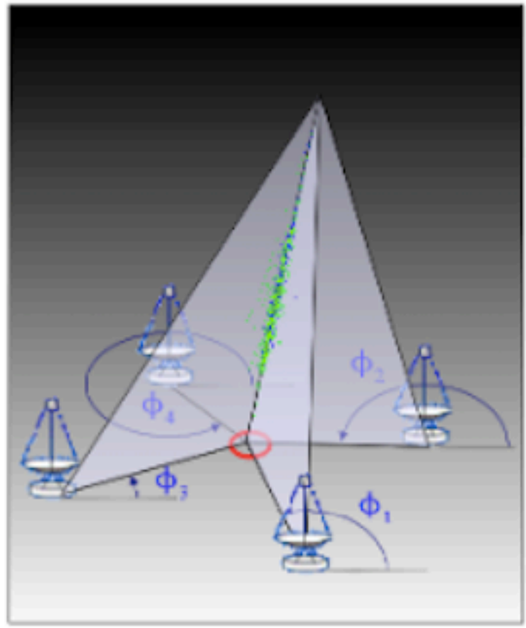

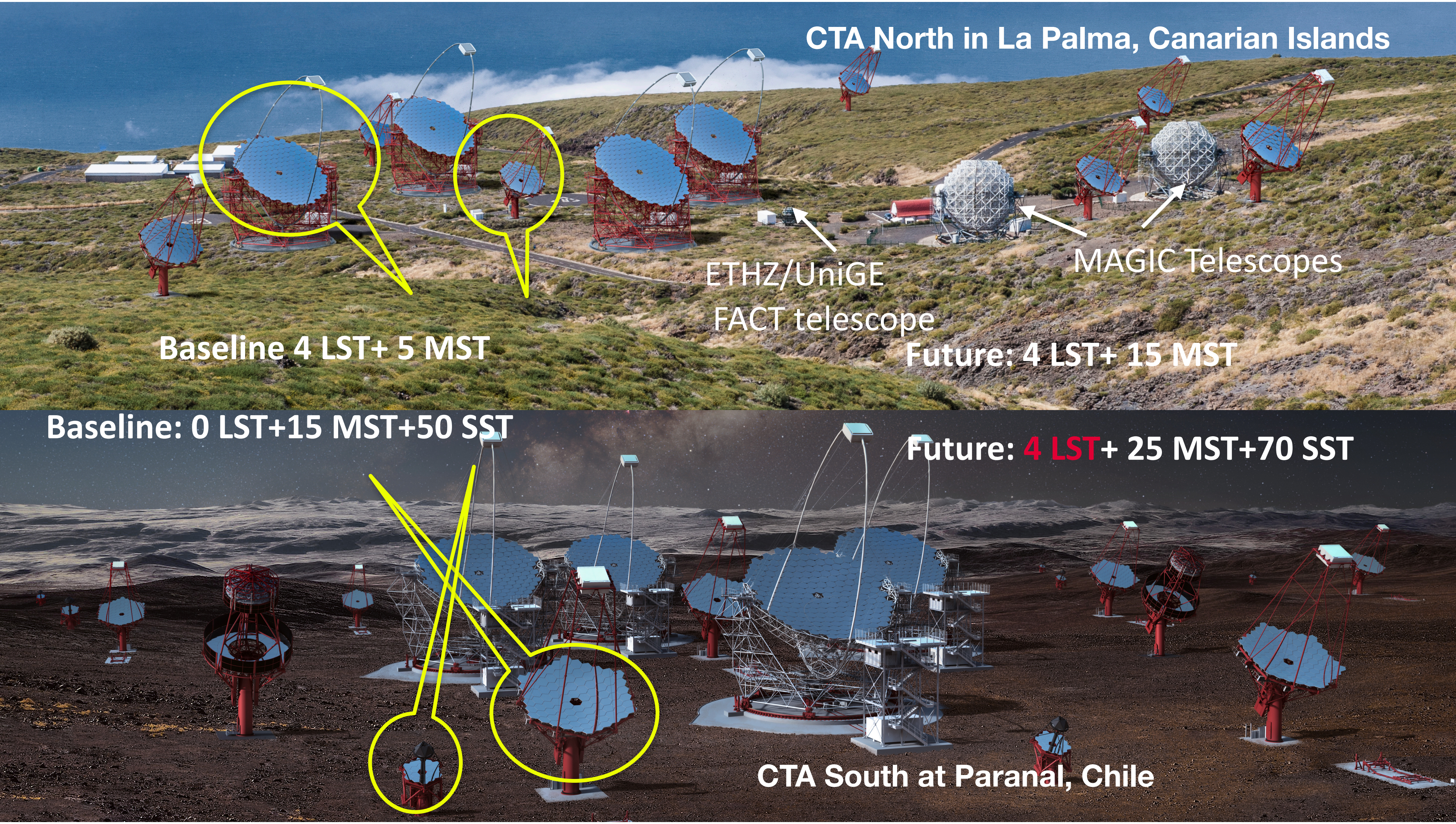

CTA North in La Palma, Canarian Islands
ETHZ/UniGE
FACT telescope
MAGIC Telescopes
Baseline 4 LST+ 5 MST
Future: 4 LST+ 15 MST
Baseline: 0 LST+15 MST+50 SST
Future: 4 LST+ 25 MST+70 SST
CTA South at Paranal, Chile

An image built from the probability density of events

γ

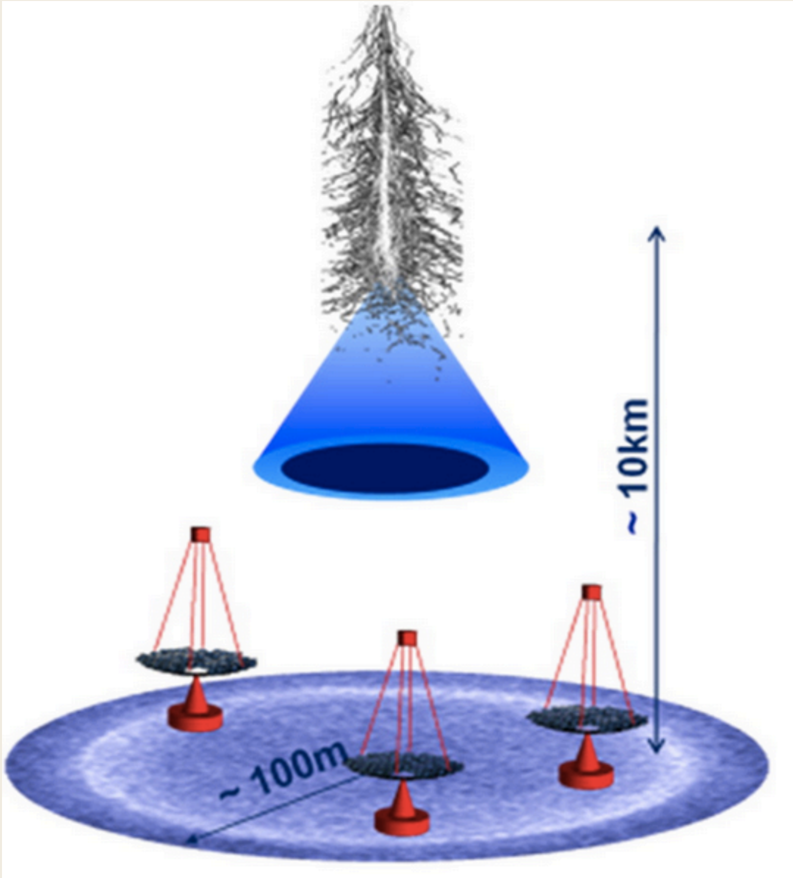

Light pool

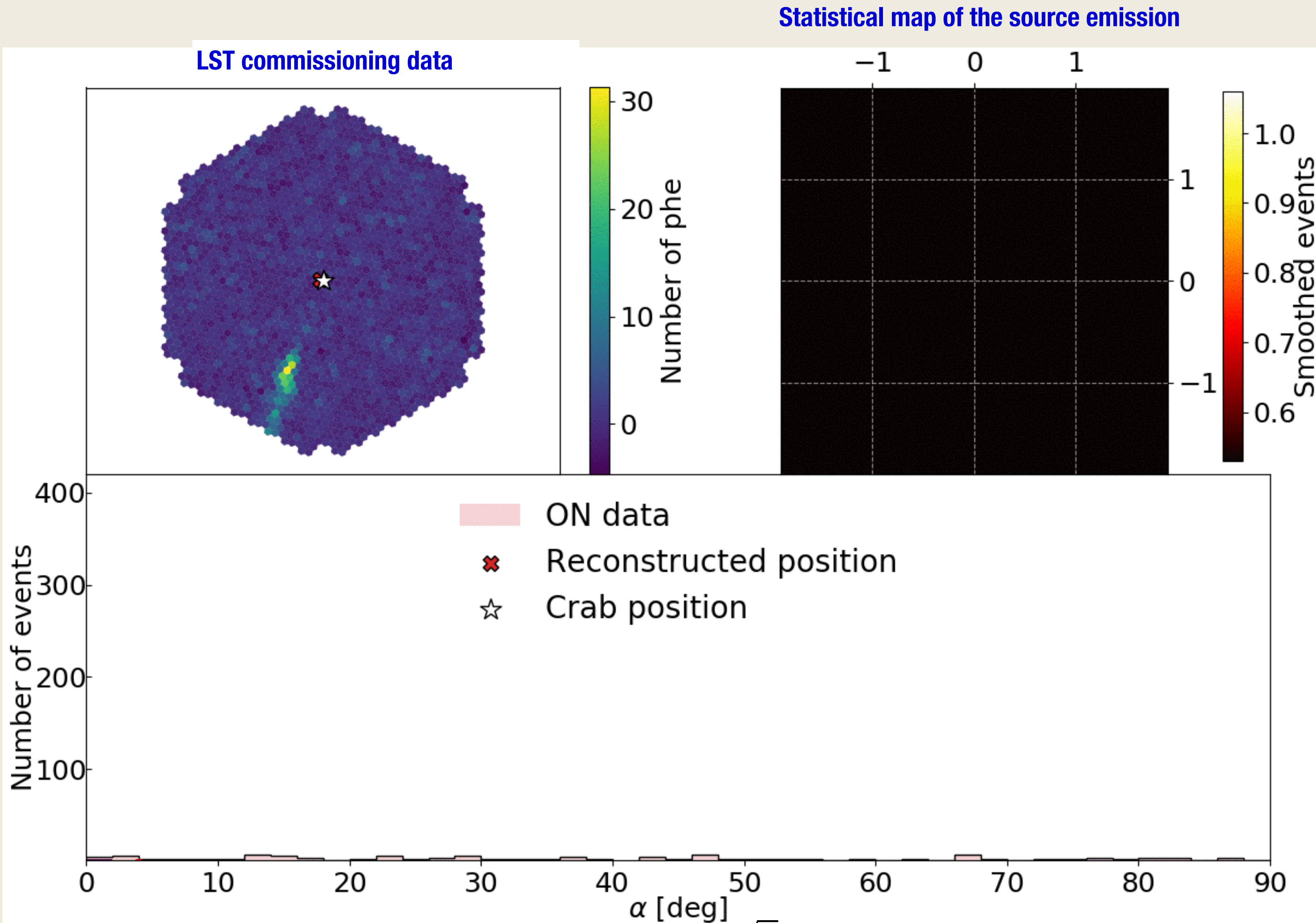

When the measurement is stereoscopic the background is largely reduced and the source is observed in a S/N regime not $S/\sqrt{N}$ and $E_{th} \propto 1/A_{mirror}$ rather than $E_{th} \propto 1/\sqrt{A_{mirror}}$

https://www.cta-observatory.org/lst1-detects-first-gamma-ray-signal/

Commissioning LST-1

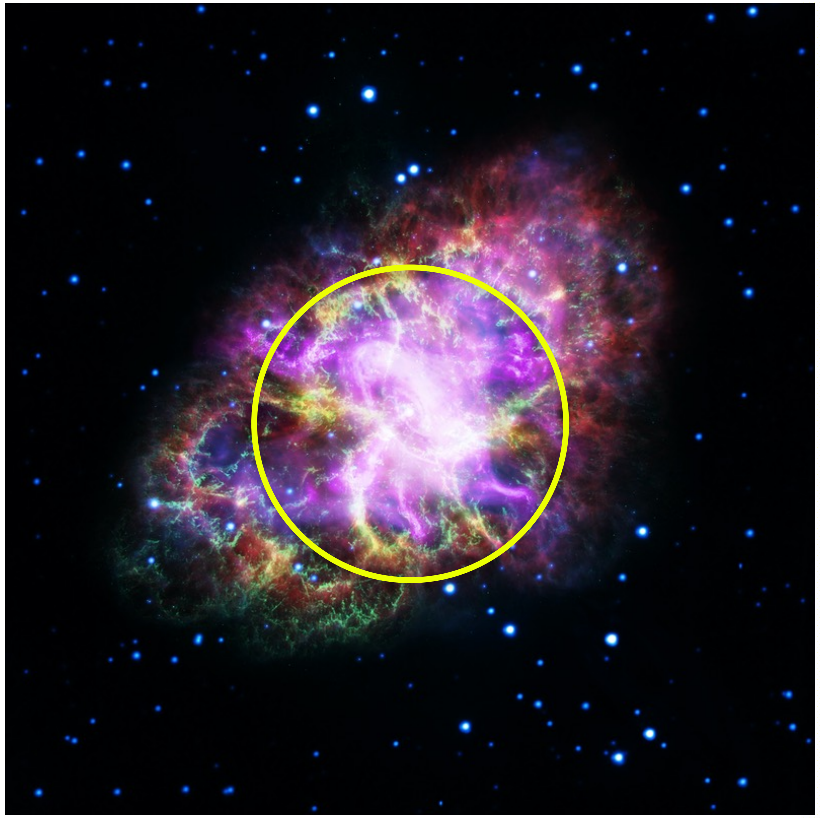

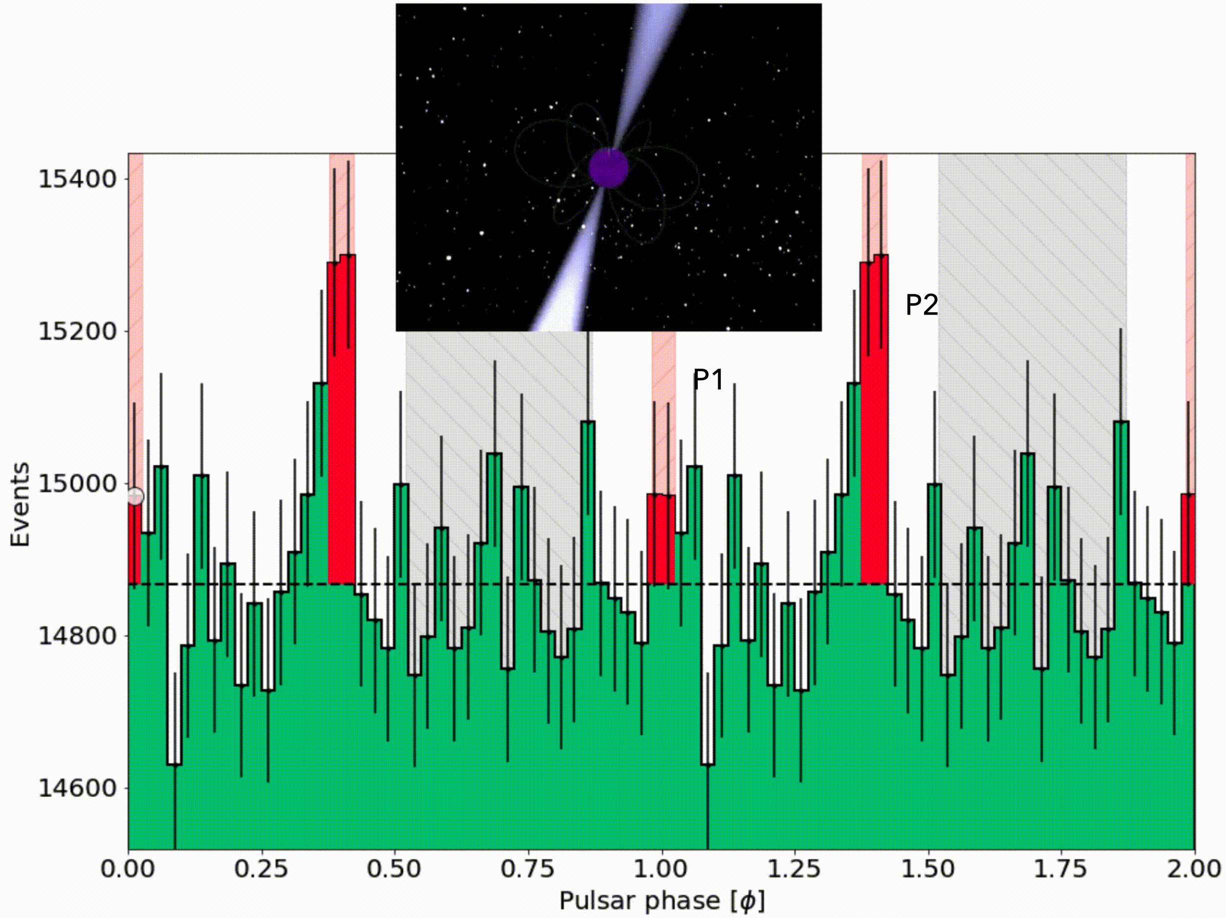

The neutron star pulsations at the centre of the Crab Nebula. P2/P1 >1 indicates a large threshold still > 100 GeV

https://www.cta-observatory.org/lst1-detects-vhe-emission-from-crab-pulsar/

The `standard candle' of gamma-ray astronomy

MAGIC data

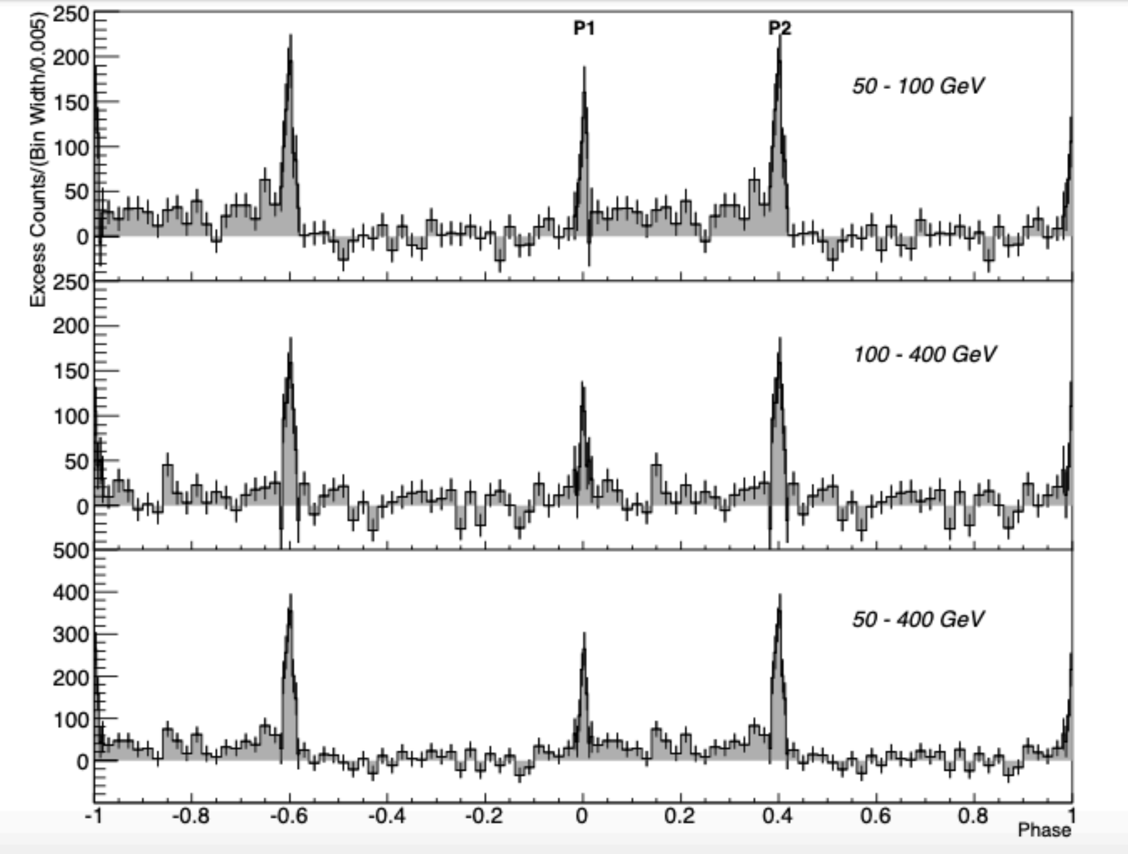

Saito et al for the MAGIC Collaboration, arXiv:1502.02757

https://arxiv.org/pdf/1510.07048.pdf 320 hours

Pulsed emission up to 1.5 TeV!

Eth > 100 GeV

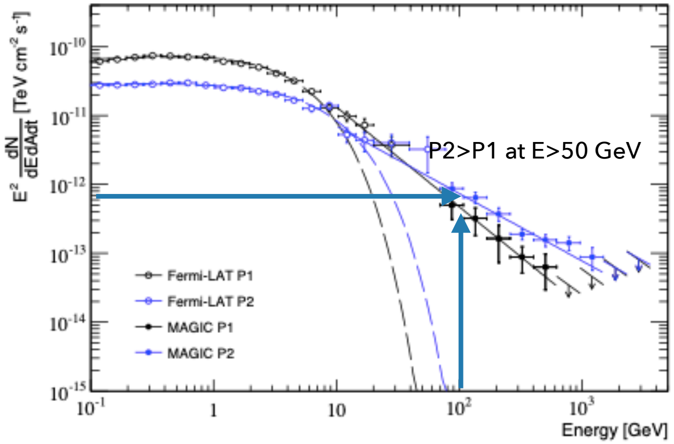

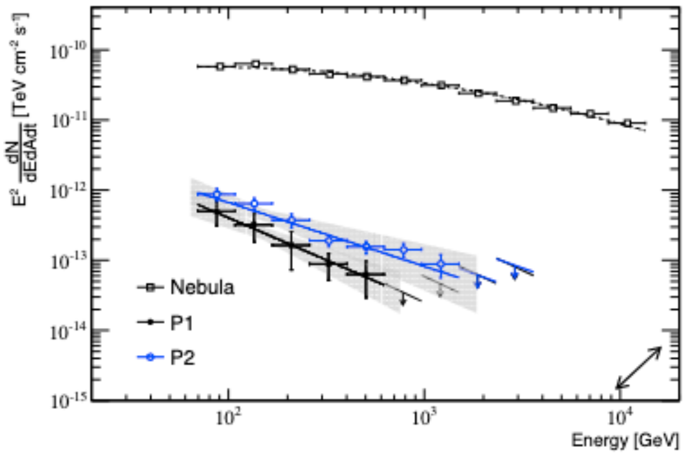

LHAASO: Large High Altitude Air Shower Observatory

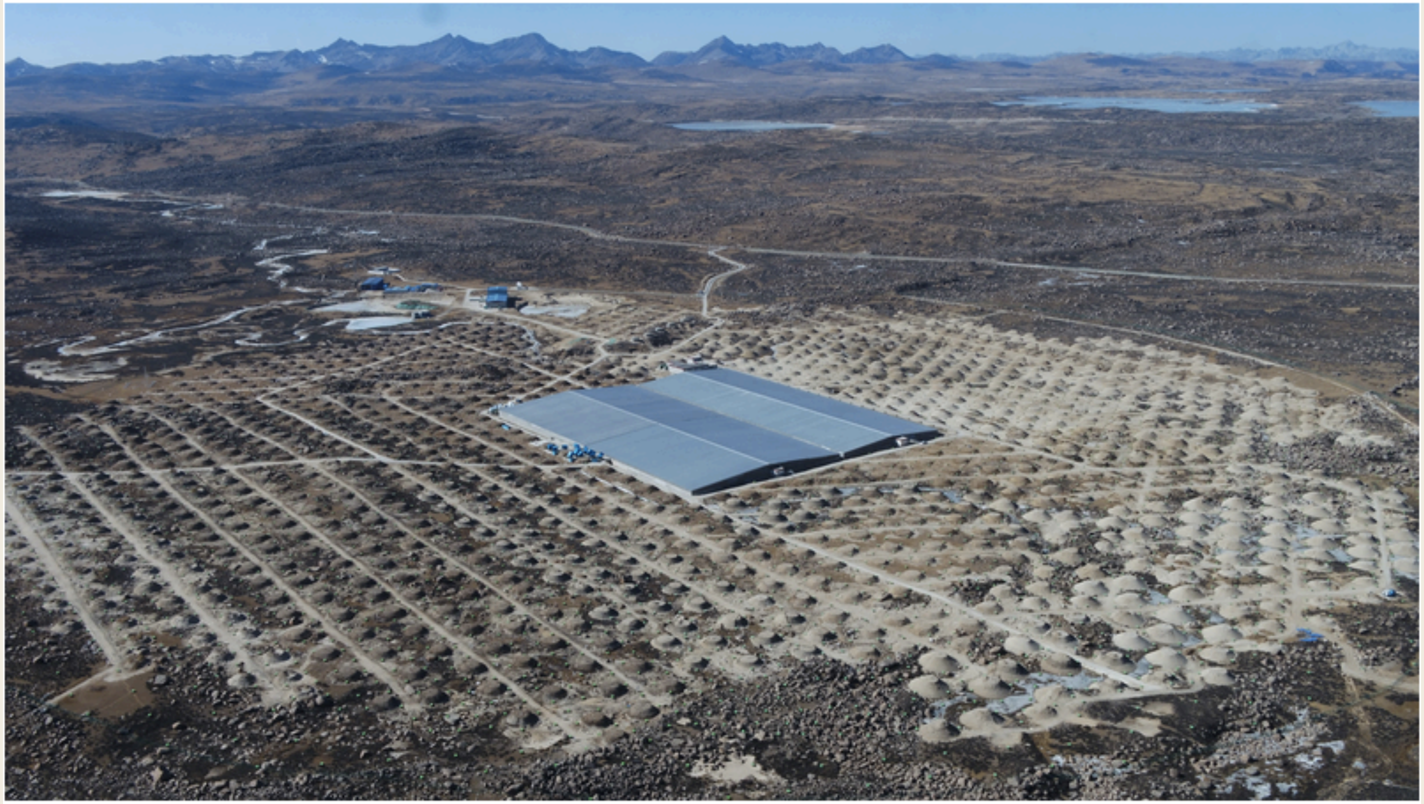

Aerial photograph of LHAASO (Image by IHEP)

Lightguides produced in Switzerland

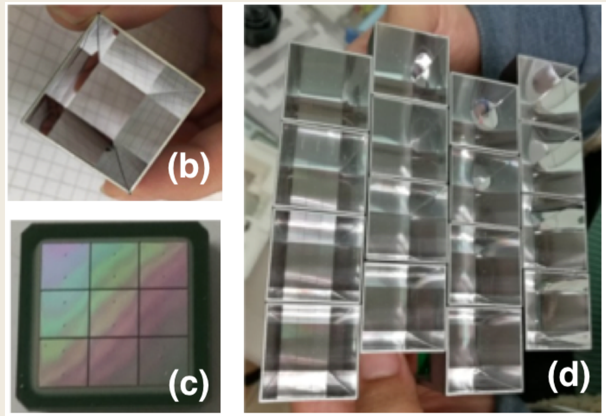

80’000 m² water pools WCDA,

~200 GeV-20 TeV and ~9mCU @ few TeV

KM2A with EM & muon detectors

> 10 TeV

UHE astronomy : Crab Nebula with LHAASO

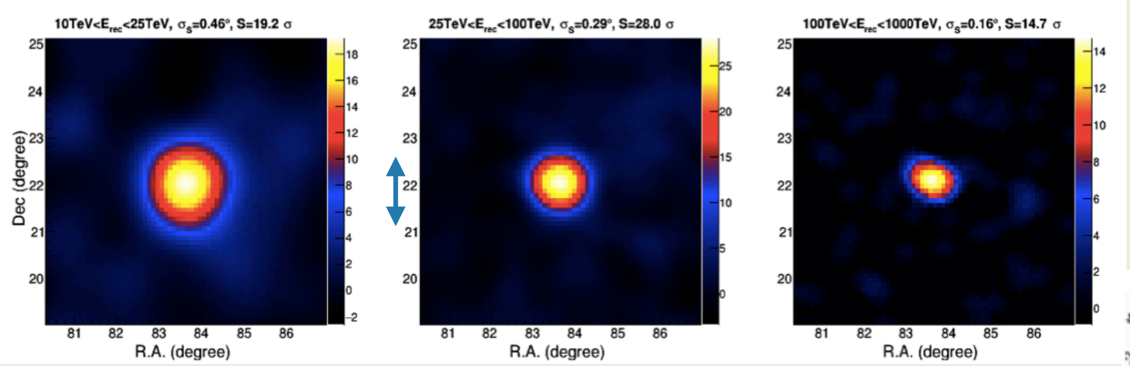

Crab Nebula image from the KM2A of LHAASO

Crab Nebula a clear PeVatron with secondary gammas > 100 TeV; also seen by HAWC and Tibet ASγ with no cut -off above 400 TeV indicating that primary electrons can reach above 0.1 PeV.

WCDA: 0.45°(<0.2°) @ 1 TeV (>6 TeV) with the pointing accuracy < 0.05°. Significance in image 4-77σ

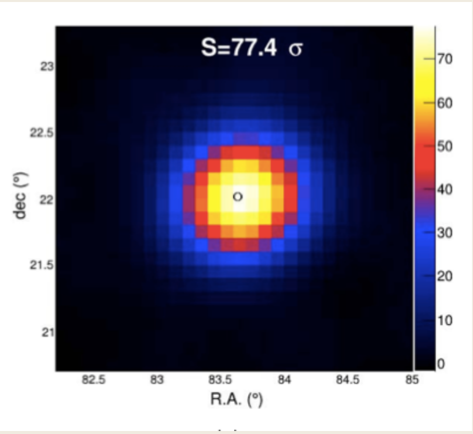

1° range

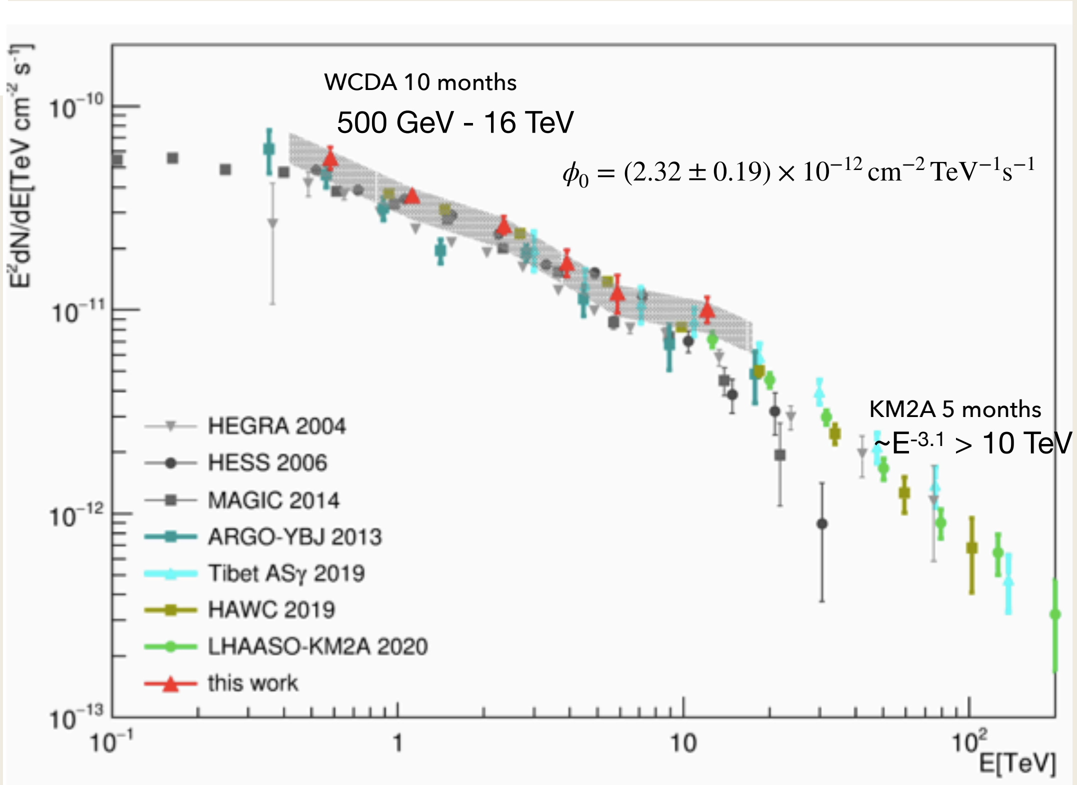

KM2A: https://arxiv.org/abs/2010.06205 , WFCDA https://arxiv.org/pdf/2101.03508.pdf

PeVatron candidates (> 100 TeV)

12 young massive star clusters and supernova remnants, PWN, 1 yet unidentified. E_{max} = 1.42 PeV for LHAASO J2032+4102 Cygnus cocoon!!)

source name	R.A. (°)	dec (°)	Significance (σ) above 100 TeV	E_{Max} (PeV)	Flux ($\pm$ error) (CU) at 100 TeV	
LHAASO J0534+2202	83.55	22.05	17.8	0.88 $\pm$0.11	1.00(0.14)	Crab Nebula 0.30°
LHAASO J1825-1326	276.45	-13.45	16.4	0.42 $\pm$0.16	3.57(0.52)	
LHAASO J1839-0545	279.95	-5.75	7.7	0.21 $\pm$0.05	0.70(0.18)	
LHAASO J1843-0338	280.75	-3.65	8.5	0.26 $^{+0.16}_{-0.10}$	0.73(0.17)	
LHAASO J1849-0003	282.35	-0.05	10.4	0.35 $\pm$0.07	0.74(0.15)	
LHAASO J1908+0621	287.05	6.35	17.2	0.44 $\pm$0.05	1.36(0.18)	MGRO 1908+06 0.58°
LHAASO J1929+1745	292.25	17.75	7.4	0.71 $^{+0.16}_{-0.07}$	0.38(0.09)	
LHAASO J1956+2845	299.05	28.75	7.4	0.42 $\pm$0.03	0.41(0.09)	
LHAASO J2018+3651	304.75	36.85	10.4	0.27 $\pm$0.02	0.50(0.10)	
LHAASO J2032+4102	308.05	41.05	10.5	1.42 $\pm$0.13	0.54(0.10)	Cygnus OB2 TeV J2032+4130
LHAASO J2108+5157	317.15	51.95	8.3	0.43 $\pm$0.05	0.38(0.09)	
LHAASO J2226+6057	336.75	60.95	13.6	0.57 $\pm$0.19	1.05(0.16)	

Image credit: Chandra, Hubble, Spitzer, NASA

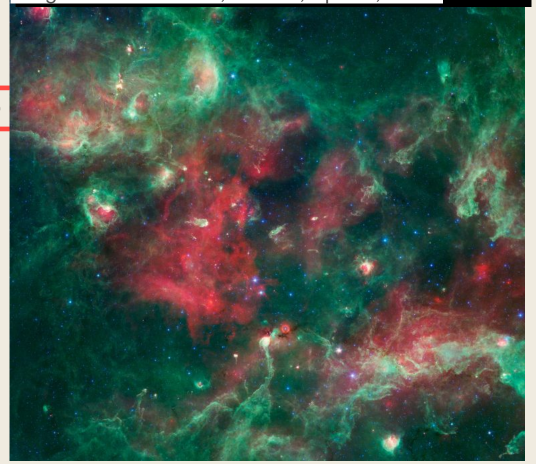

Image credit: NASA/JPL-Caltech/Harvard-Smithsonian CfA

`…photons exceeding 1 PeV from it, can be treated as evidence of the operation of massive stars as hadronic PeVatrons. The leptonic (IC) origin of radiation can be excluded because of the lack of brightening of the -ray image towards Cygnus OB2. A decisive test for the acceleration of protons, presumably via collisions of the stellar winds, and continuous injection into the circumstellar medium over million-year timescales, would be the derivation of hard injection spectra and radial dependence of the density of UHE protons'

Nature paper (press release on May 17): Detection of Ultra-high Energy Photons up to 1.4 PeV from 12 Gamma-ray Sources

MGRO J1908+06

Leptonic : 6% spin-down power of PSR J1907+0602 in in $e^{\pm}$ with injection spectrum $E^{-1.75}exp[-(E_e/800\,\mathrm{TeV})^2]$
Hadronic models : parent protons with spectrum $E^{-1.85}exp[-E/380\,\mathrm{TeV}]$ (solid line) or broken power law with $E^{-1.2}$for E< 25 TeV and $E^{-2.7}$ for E>25 TeV and cut-off at 1.3 PaV (heavy solid line)

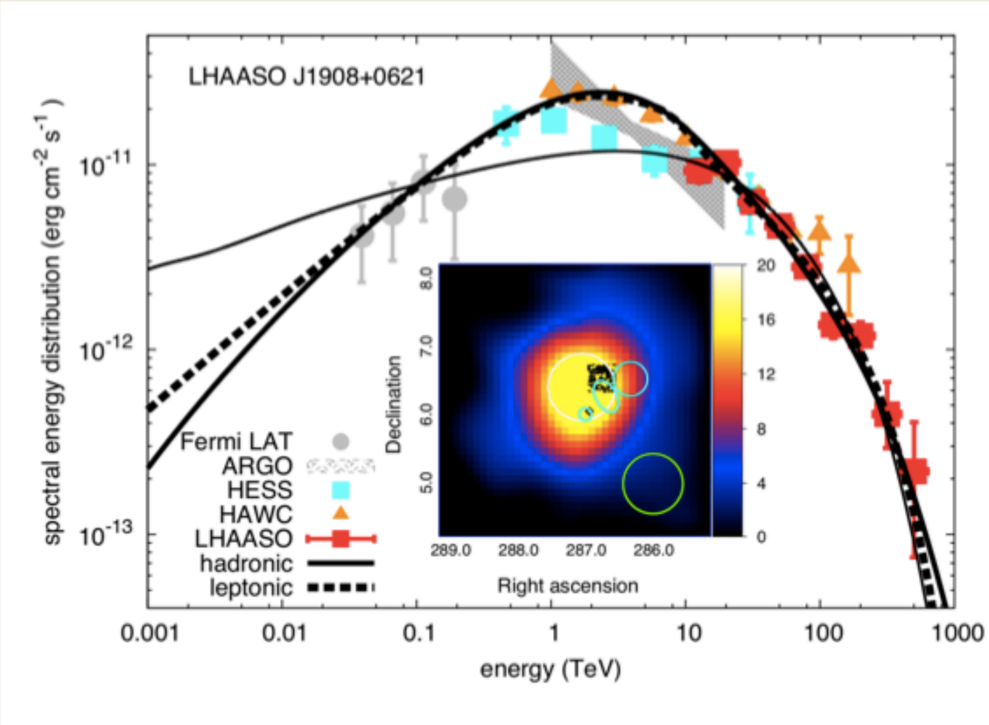

Ali Kheirandish

arxiv:2006.16087

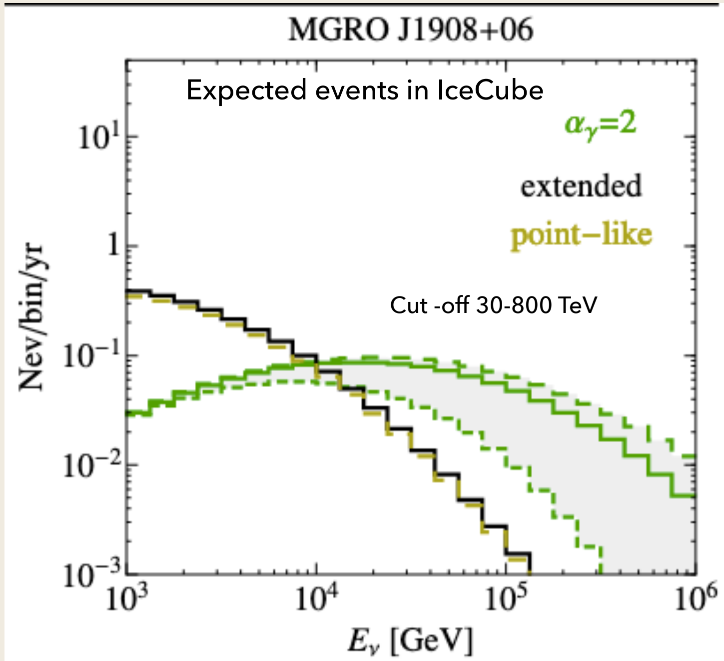

~18σ from LHAASO 1908+0621 (coincident with MGRO 1908+06) with E_{max} ~440 TeV

IceCube observed a 2% excess from a stacking analysis of Milagro hot spots including MGRO 1908+06 (arxiv:1406.6757 & PhD Thesis Rameez UNIGE) nd Cyg OB2.

PWN are only leptonic? Star forming regions, SNR shocks &Molecular clouds

Cosmic ray origin and acceleration

Cosmic rays are caused by exploding stars which burn with a fire equal to 100 million suns and then shrivel from ½ million mile diameters to little spheres 14 miles thick, says Prof. Fritz Zwicky, Swiss Physicist

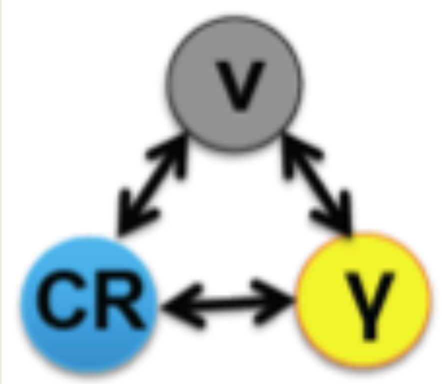

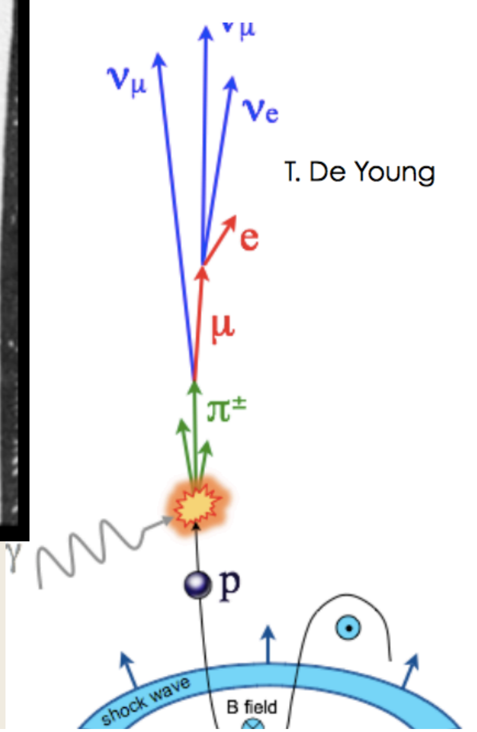

T. De Young

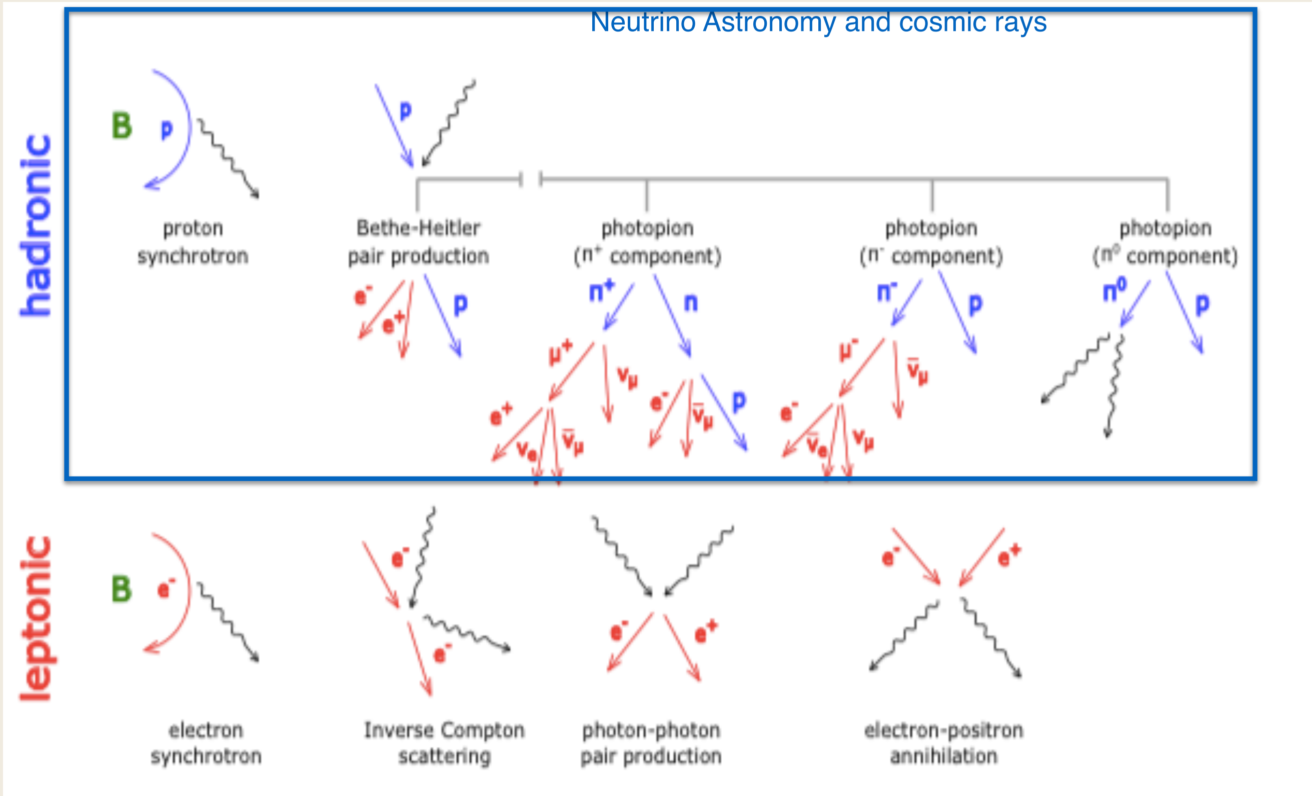

Image from Petropolou et al, 2016

HADRONIC SIGNATURES IN SPECTRAL EMISSION DISTRIBUTION

energy flux $E^2\, d/dE \sim \nu F(\nu)$

synchrotron radiation from electrons
$dE/dt_{Sy} = k\, \gamma_e^2\, U_{mag} \sim \gamma_e^2\, B^2$

Inv. Compton scattering by the same electrons
$dE/dt_{IC} = k\, \gamma_e^2 U_{rad}$

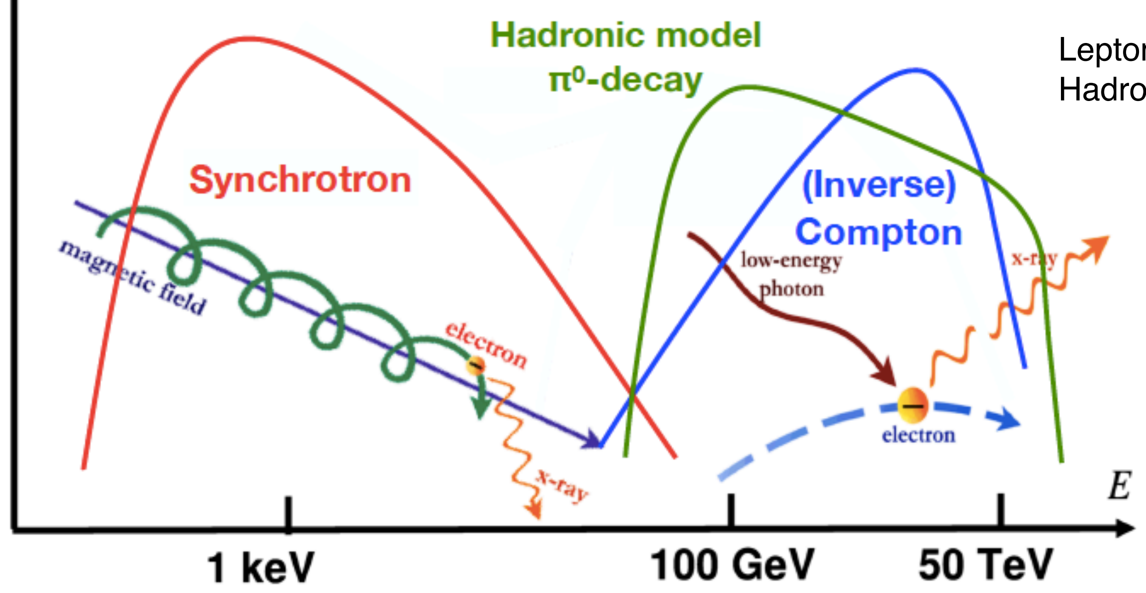

Leptonic scenario: red and blue
Hadronic scenario: pion decay

Fermi, Science 2013

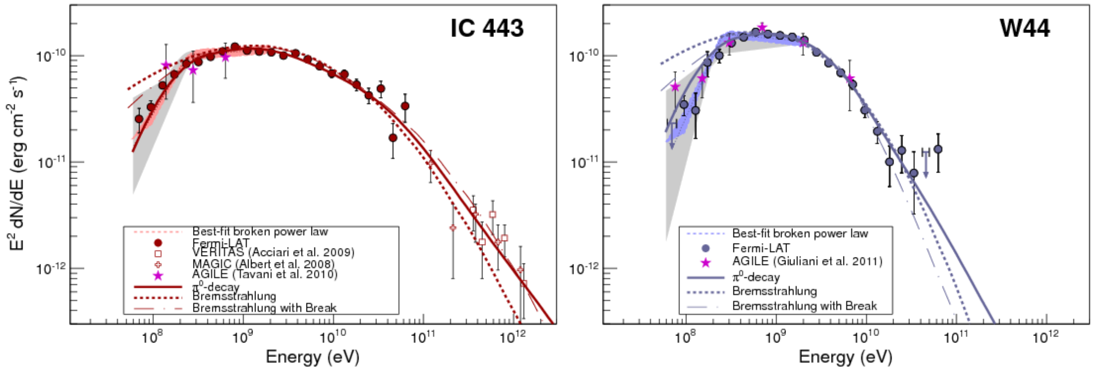

Synchroton losses of protons are about 10^{-6} the ones of electrons!

Gamma-ray sources from space: 10 GeV-100GeV

Fermi 8 yr catalogue (4FGL) 50 MeV - 300 GeV 5064 sources, 62% blazars, 1.5% 2.7% SNR & PWN, 4.7% Pulsars

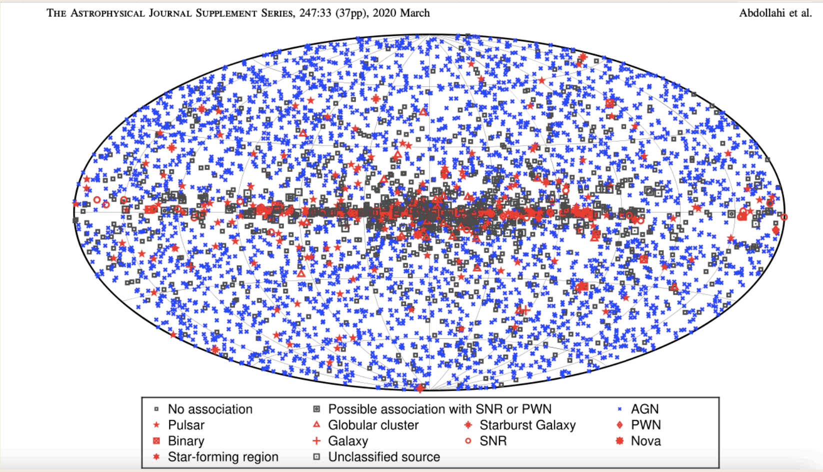

Space based detectors

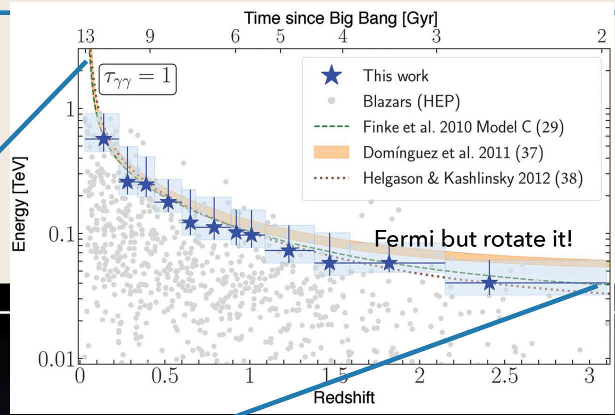

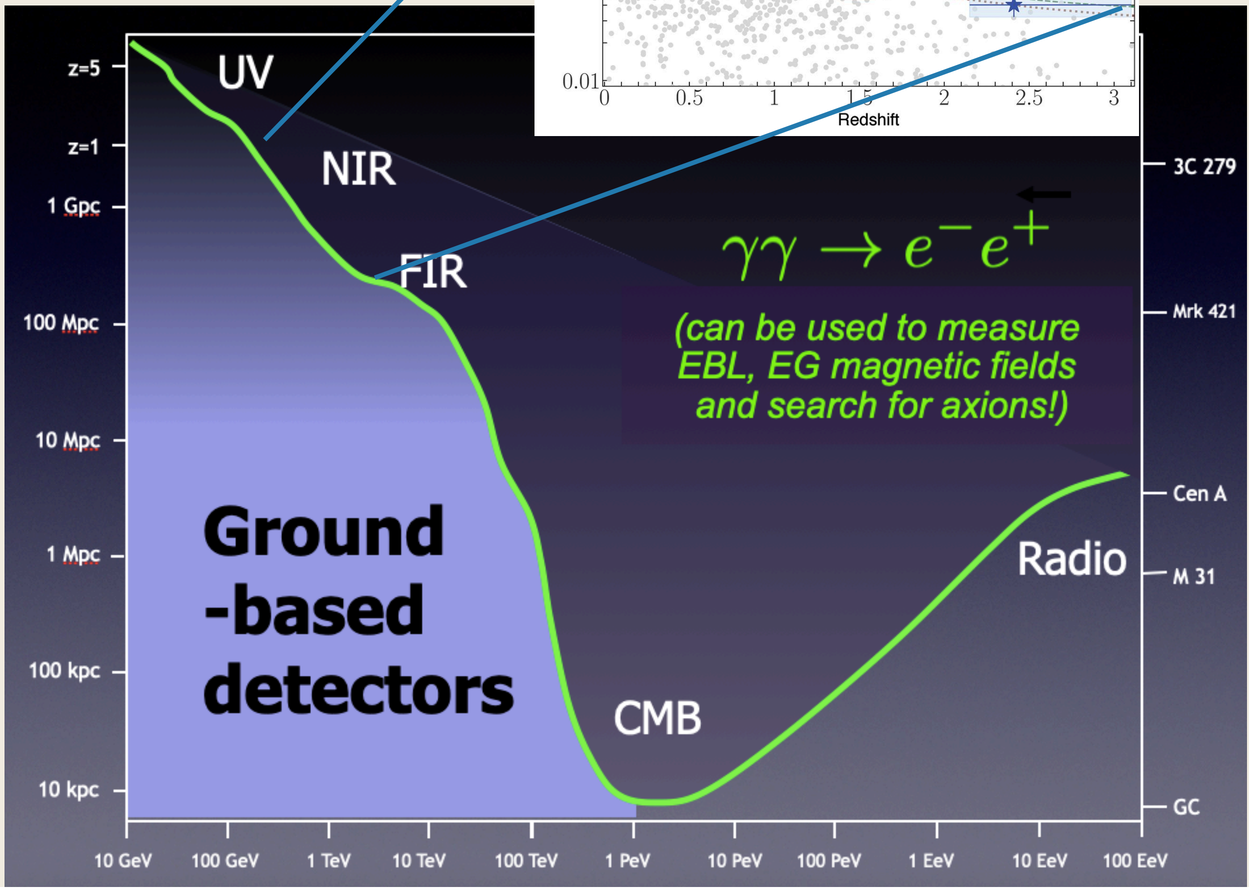

Gamma-ray sources from ground

https://github.com/sfegan/kifune-plot

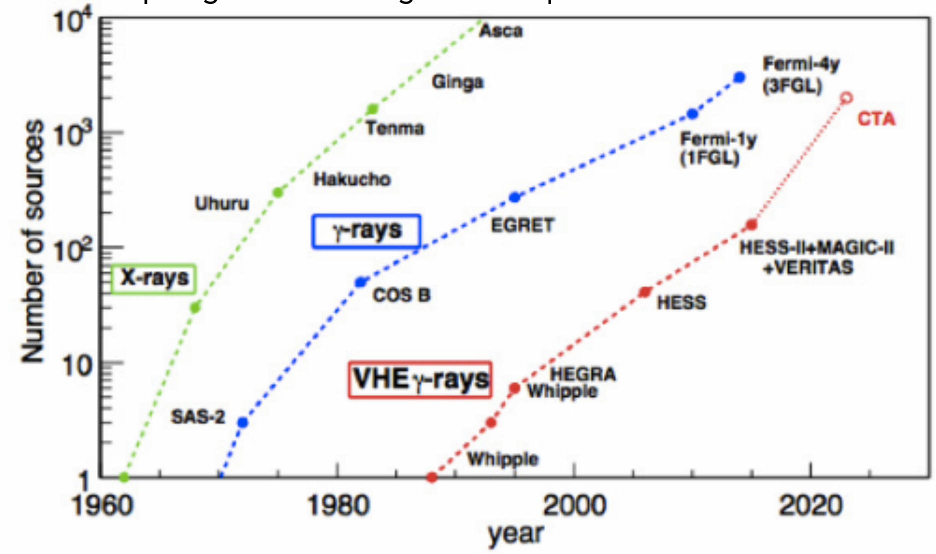

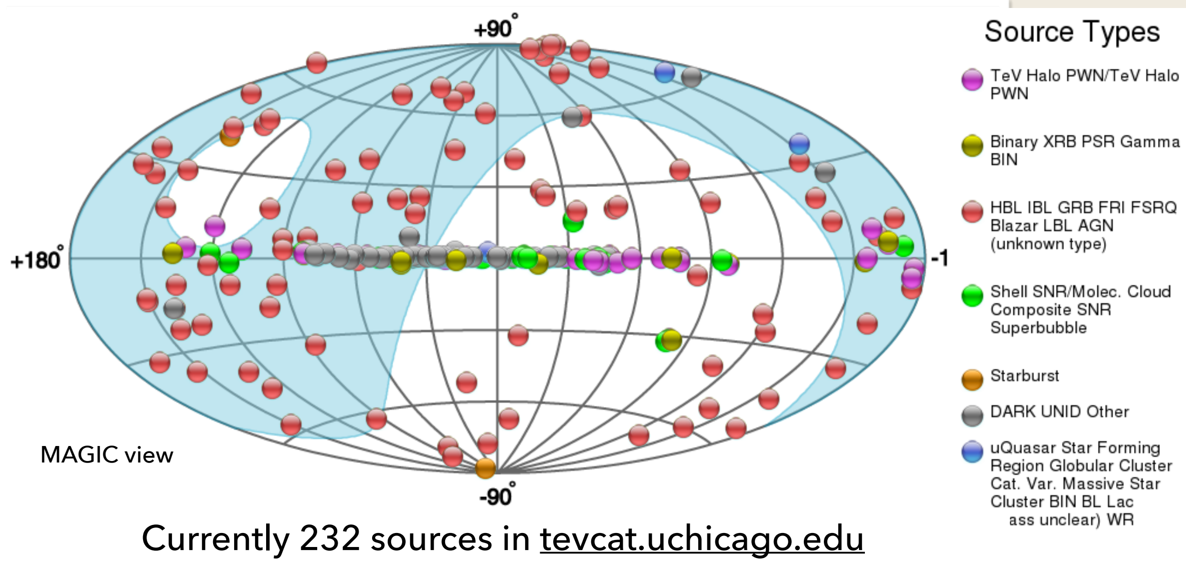

Currently 232 sources in tevcat.uchicago.edu

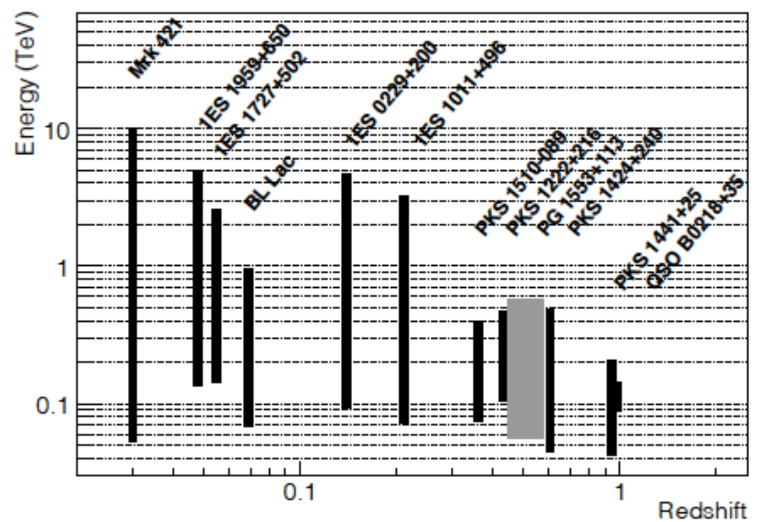

12 blazars in the redshift range z = 0.03 to 0.944, obtained by the MAGIC telescopes and Fermi-LAT (arXiv:1904.00134)

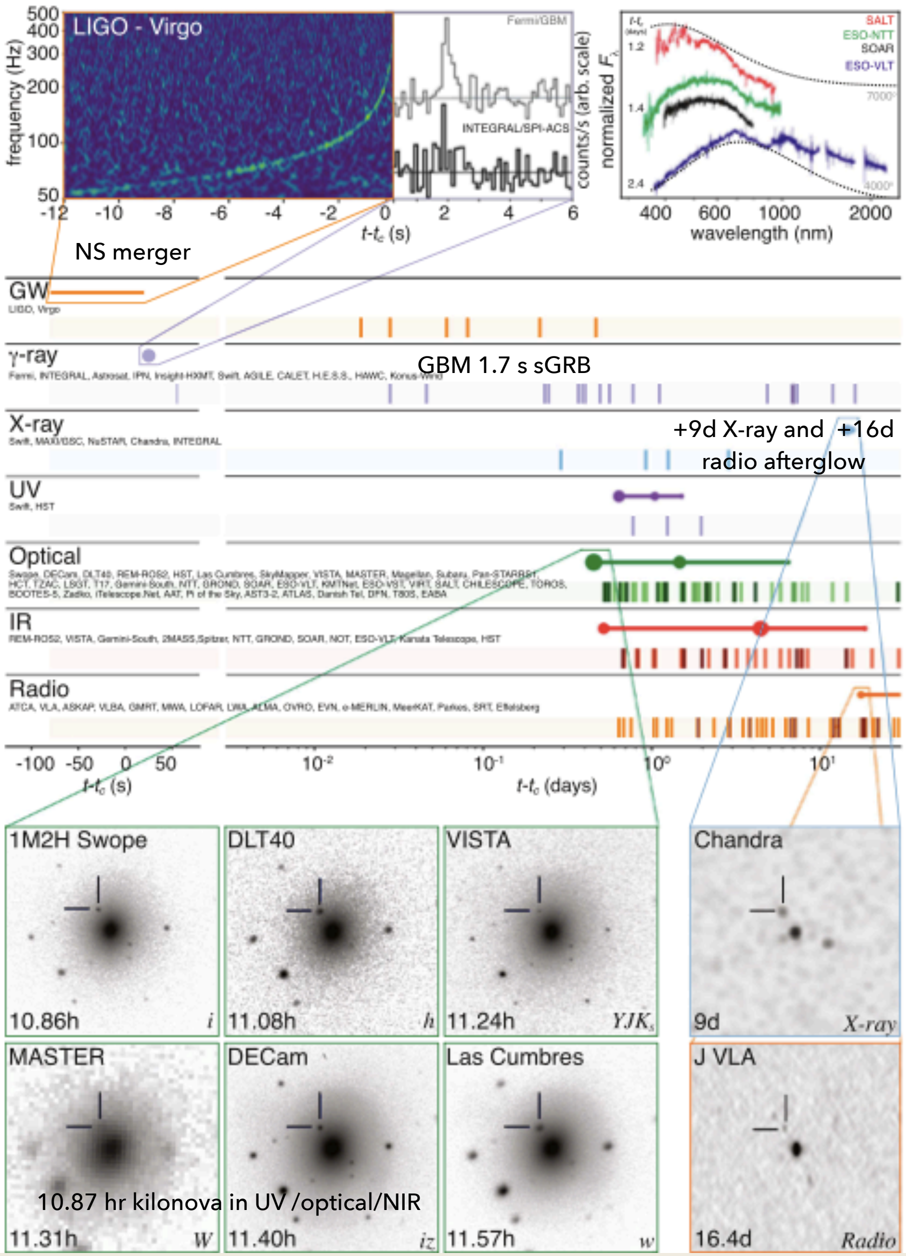

The multi-messenger event!

GW 170817 - photon connection

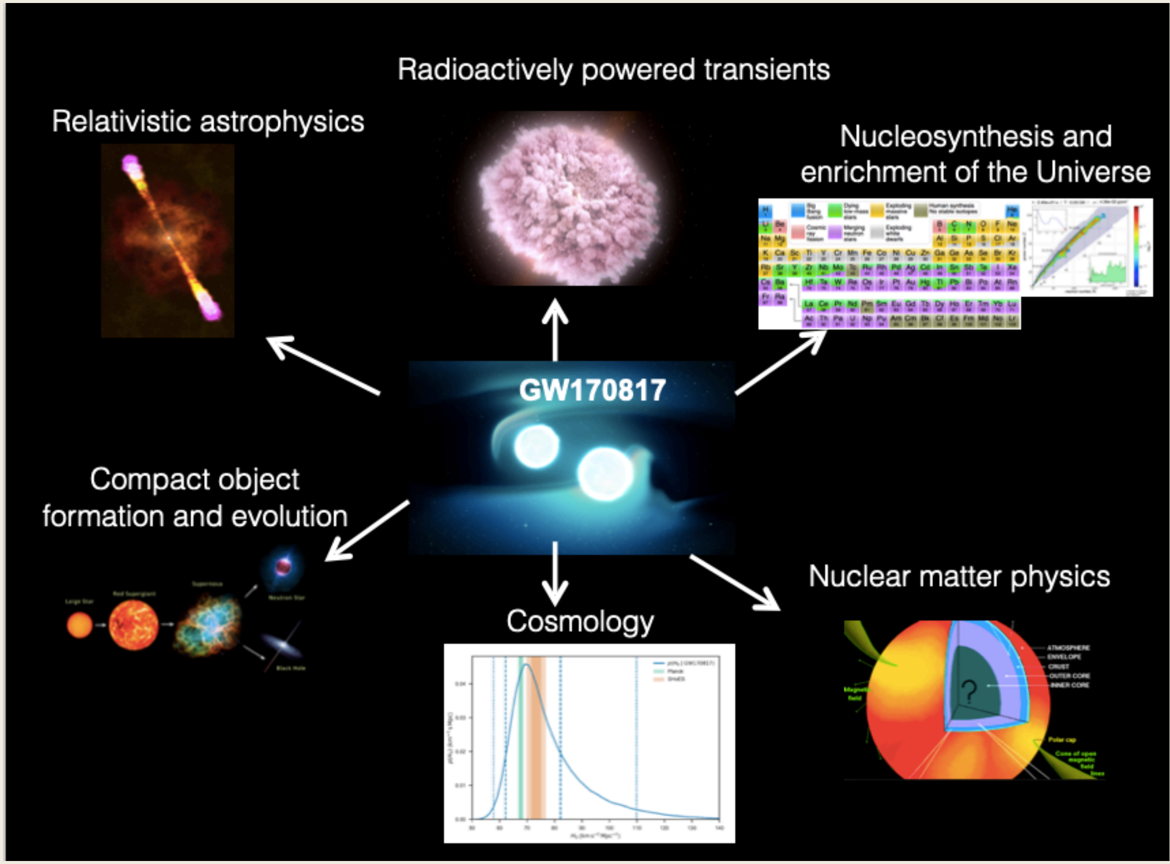

Figure from M. Branchesi's presentation at Neutrino Telescopes 2021

GSSI Colloquia: A. Bonanno and M.Maggiore this year

A likelihood analysis for IceCube

$$\mathcal{L}(\vec{n}_s, \vec{\gamma}, \vec{t}_0, \vec{\sigma}_T) = \prod_{i=\text{events}} \left\{ \sum_{f=\text{flares}} \left[\frac{n_s^{(f)}}{N} S_i^{(f)}(\gamma^f, t_0^f, \sigma_T^f) \right] + \left(1 - \sum_f \frac{n_s^{(f)}}{N} \right) B_i \right\}$$

Energy PDF

Signal: power-law $\propto E^{-\gamma^f}$

Background: data-driven

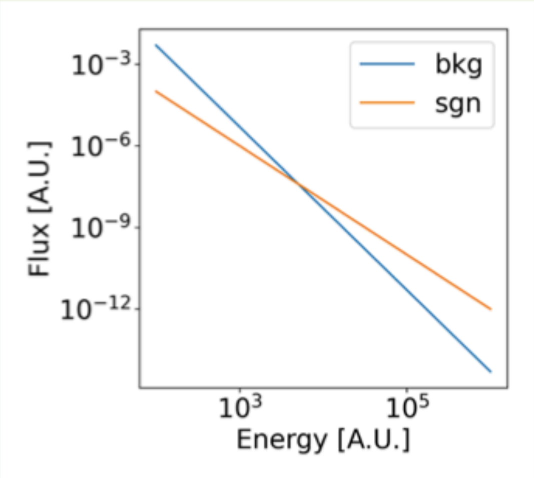

×

Spatial PDF

Signal: 2D Gaussian $\frac{1}{2\pi\sigma_i^2} \exp\left[-\frac{|\vec{x}_i - \vec{x}_S|^2}{2\sigma_i^2}\right]$

Background: data-driven

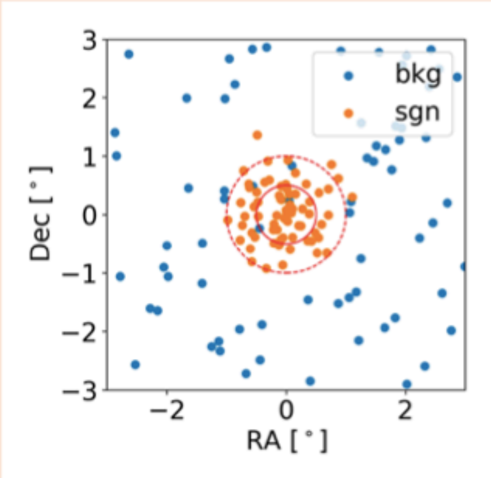

×

Time PDF

Signal: Gaussian $\propto \exp\left[\frac{(t_i - t_0^f)^2}{2\sigma_T^{f2}}\right]$

Background: uniform

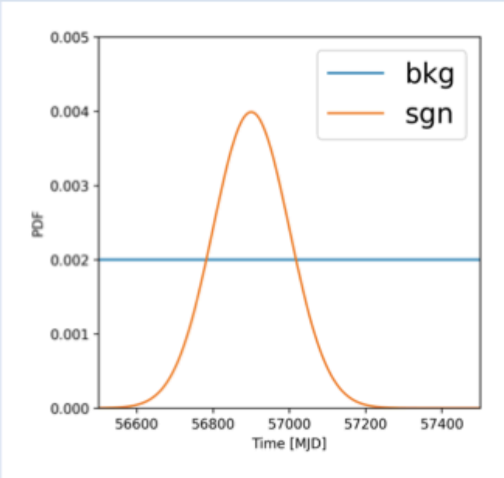

Photon - neutrino

M.G. Aartsen et al. *Science 361*

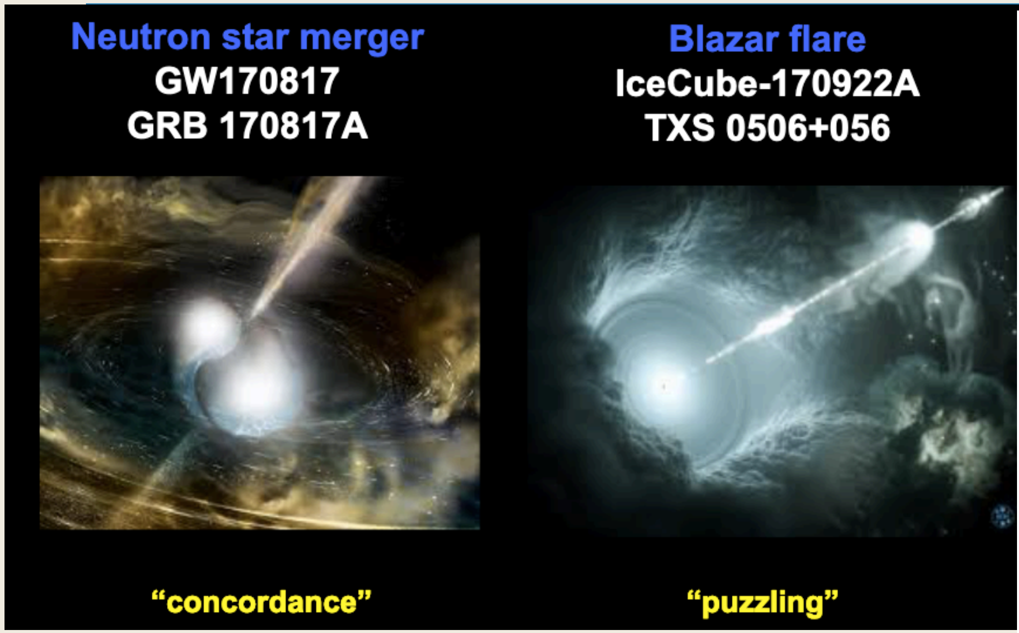

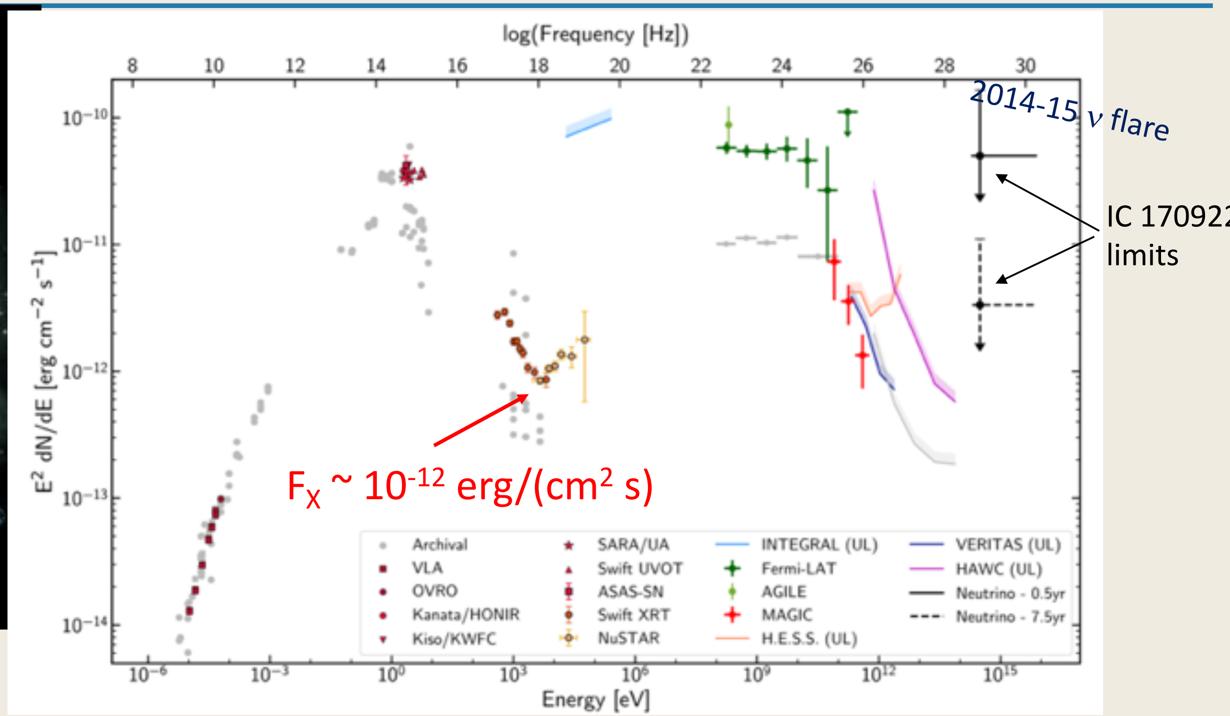

K. Murase Neutrino Telescope 2021

- The source during the flares is a **beam dump** or **opaque source** or **hidden source** not a BL Lac! At the maximum of their neutrino emitting efficiency, an **a typical blazar** may not be an efficient gamma-emitter
- Single zone models cannot explain the result

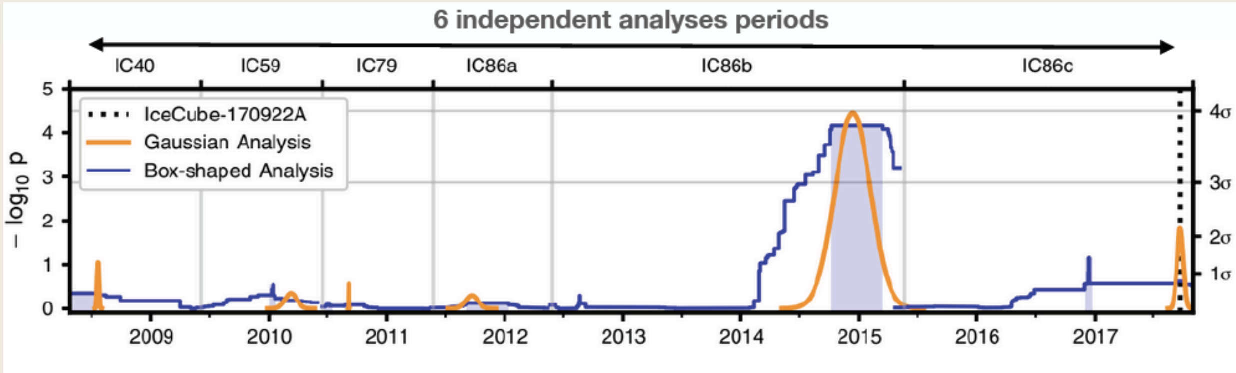

F. Halzen's and A. Franckowiak's colloquia

Asen Christov, PhD Thesis UNIGE

Puzzling…not explained by single-zone models

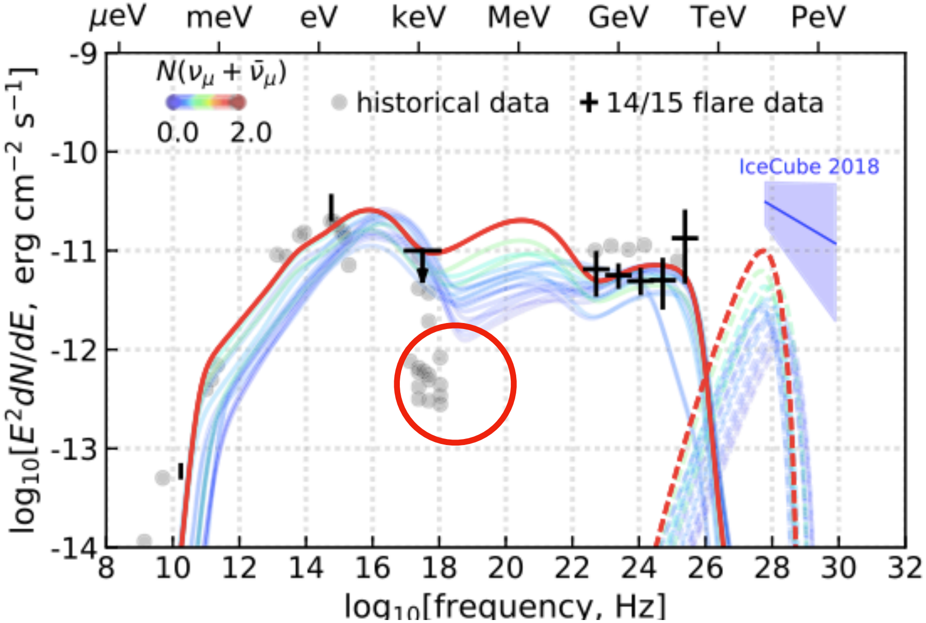

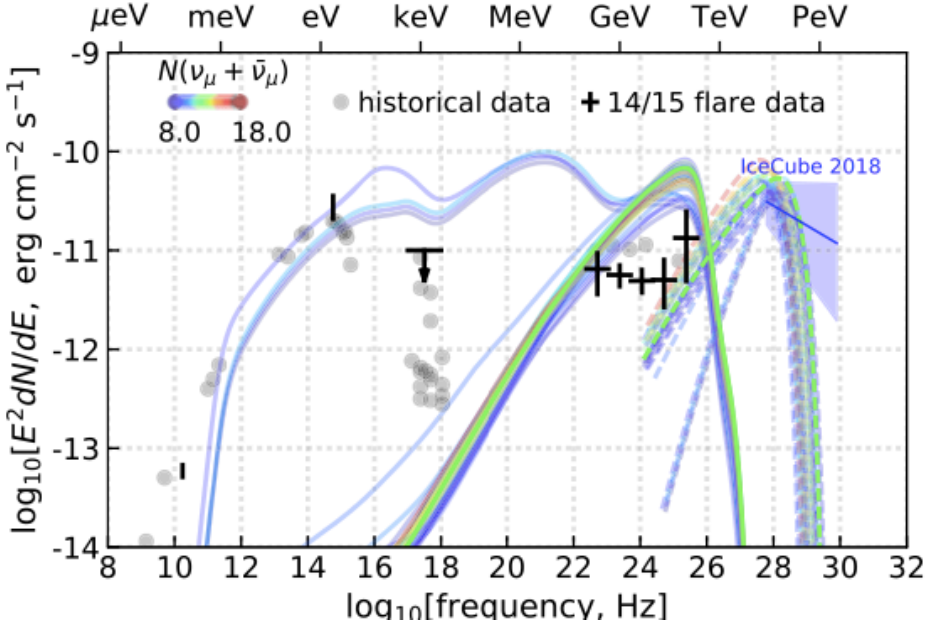

The 2014/15 ν flare poses problems to single-zone models:

- **Purely leptonic models** provide good fits but **cannot explain** νs

-**Hadronic models:** photons from π^0 and neutrinos from $\pi^{\pm}$

Left) if MWL data are considered, the SED cannot explain the observed high flux in the 2014/15 flare.

Right) if the parameters are tuned to fit the IceCube data, the X-ray flux at ~10^{-11-12} erg cm^{-2} s^{-1} is overshoot since an efficient em cascade and electron synchrotron emission is not preventable.

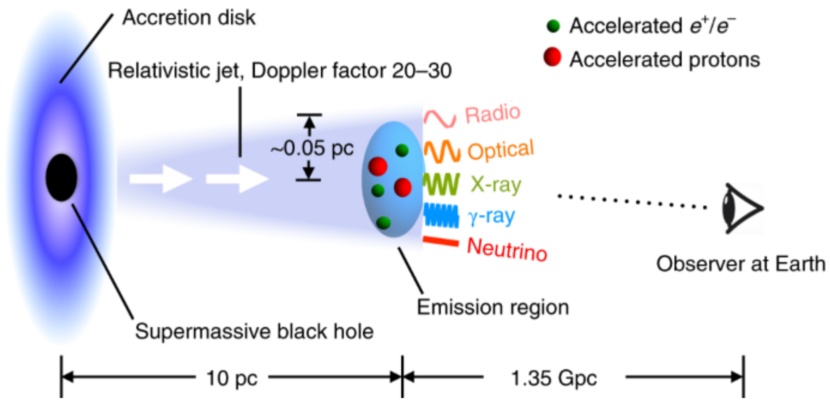

Rodrigues et al. ApJL 874 2019, A. Reimer et al. ApJ 881 2019,
F. Halzen et al. ApJL 874 2019 A. Frankowiack's talk

Gao et al. Nature Nov. 2018

Keivani et al. Nature Nov. 2018

Seyfert II galaxy: NGC1068

Tessa Carver PhD thesis UNIGE Neutrino Telescopes 2019
PhysRevLett.124.051103

IceCube 10 year data: 1) Hottest source in a 110 source catalogue (2.9σ) coincident with all sky hot source 2) Population study of the catalogue: 3.3σ Including TXS 0506+056

NGC 1068: the neutrino emission can be produced in the vicinity of the supermassive black hole in the center of the galaxy, namely in the **corona, an optically thick environment.**
A large optical depth of gamma rays requires the presence of a **compact and dense** X-ray target of keV photons

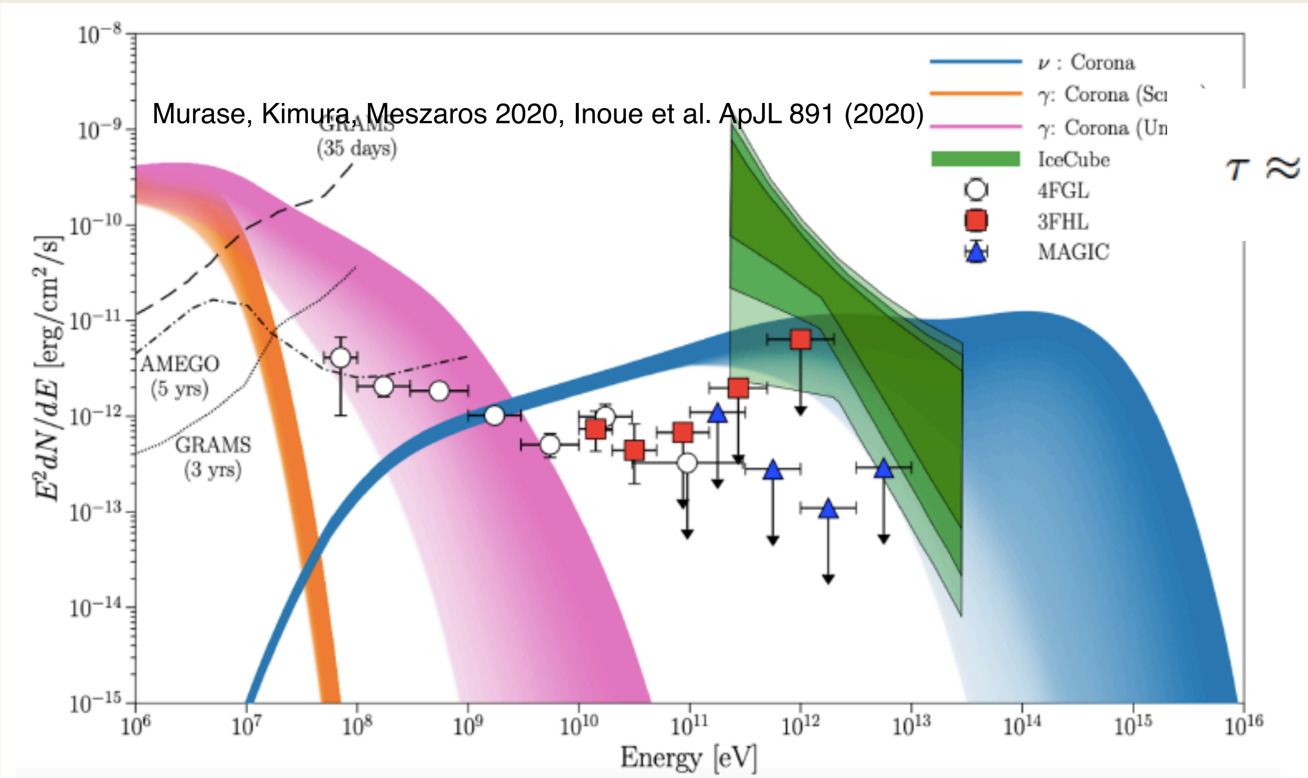

Murase, Kimura, Meszaros 2020, Inoue et al. ApJL 891 (2020)

$$\tau \approx \frac{\sigma_{\gamma\gamma}}{4\pi c}\epsilon_X^{-1} L_X R^{-1} \simeq 10^5 \left(\frac{\epsilon_X}{1\ \mathrm{keV}}\right)^{-1} \frac{L_X}{L_{\mathrm{Edd}}} \frac{R_s}{R}$$

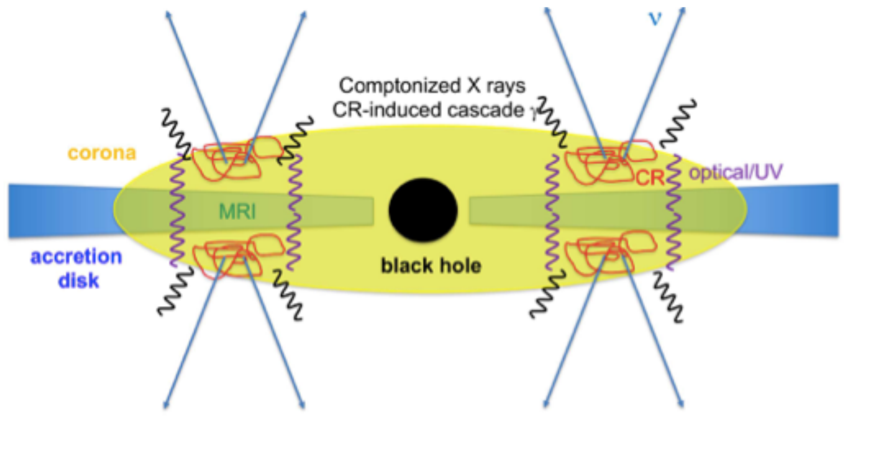

Multi-flare analysis results

F. Lucarelli Neutrino Telescopes 2021

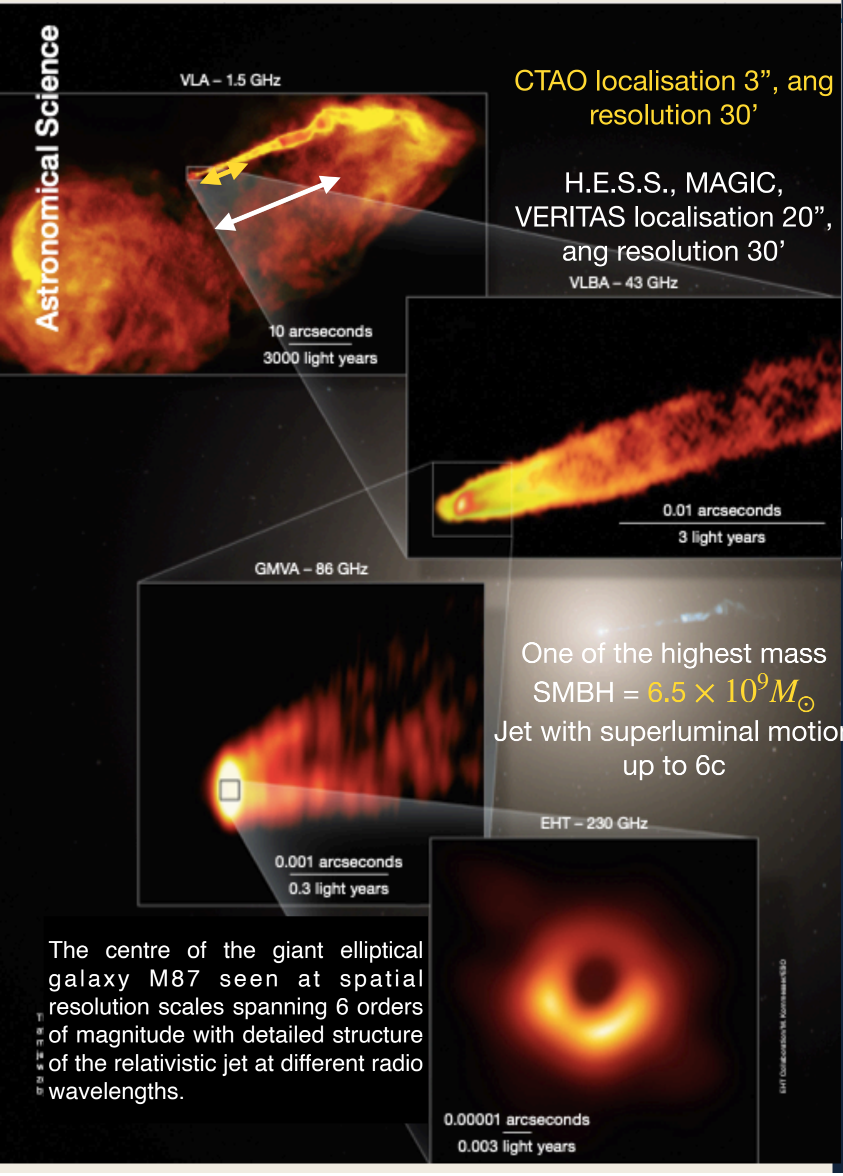

North

3.0σ post-trial from 4 sources:
M87, NGC 1068, TXS 0506+056, GB6 J1542+6129

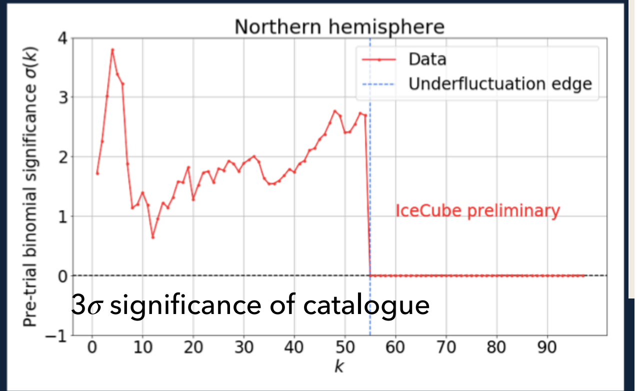

Significance of the binomial p-value in the northern hemisphere

3 TeV neutrino events in ~15 min on 57730 (Dec. 8 2016) ; M87 is hottest source.

Largest close by BH: $\sim 10^9 M_\odot$, structured jet with superluminal motion to 6c, 2d variability measured by H.E.S.S:)
Spine - sheat model by Tavecchio & Ghisellini, 2018, 2005
CTAO will have an excellent sensitivity to short flares of minute-day-scale
Structured jet

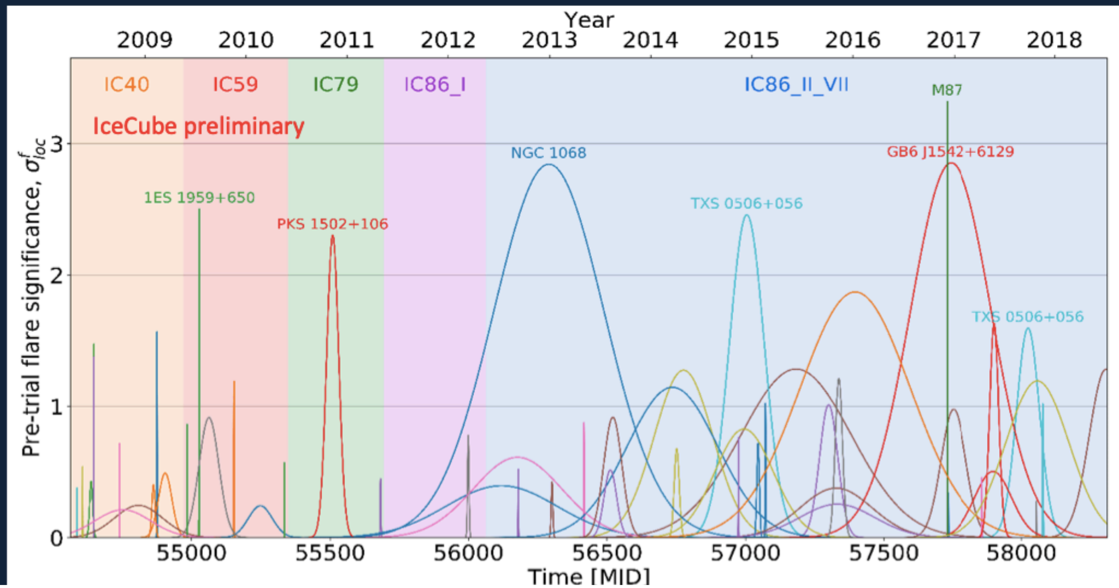

Best-fit flares of th
sources of the catalog
pre-trial flare significa

Radiation/particles from the universe

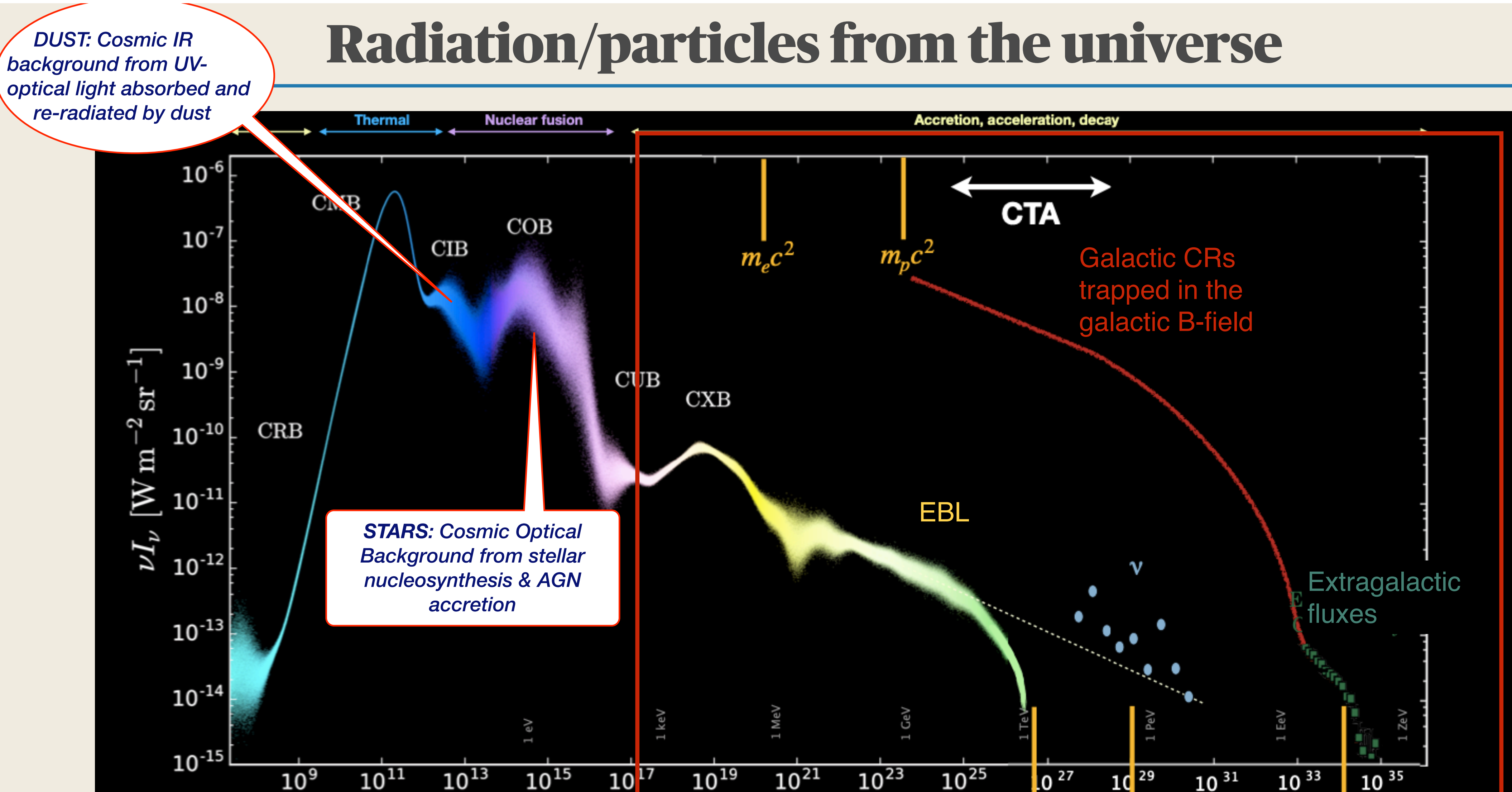

The extragalactic background light is a tracer of the star formation processes across the Universe

R. Walter adapted from De Angelis & Mallamaci, 2018

Cosmology with EBL (despite $z \lesssim 1.5-2$)

Electron positron pair production by gamma-ray interaction on Extragalactic Background Light attenuates the spectra of gamma-ray extragalactic sources.

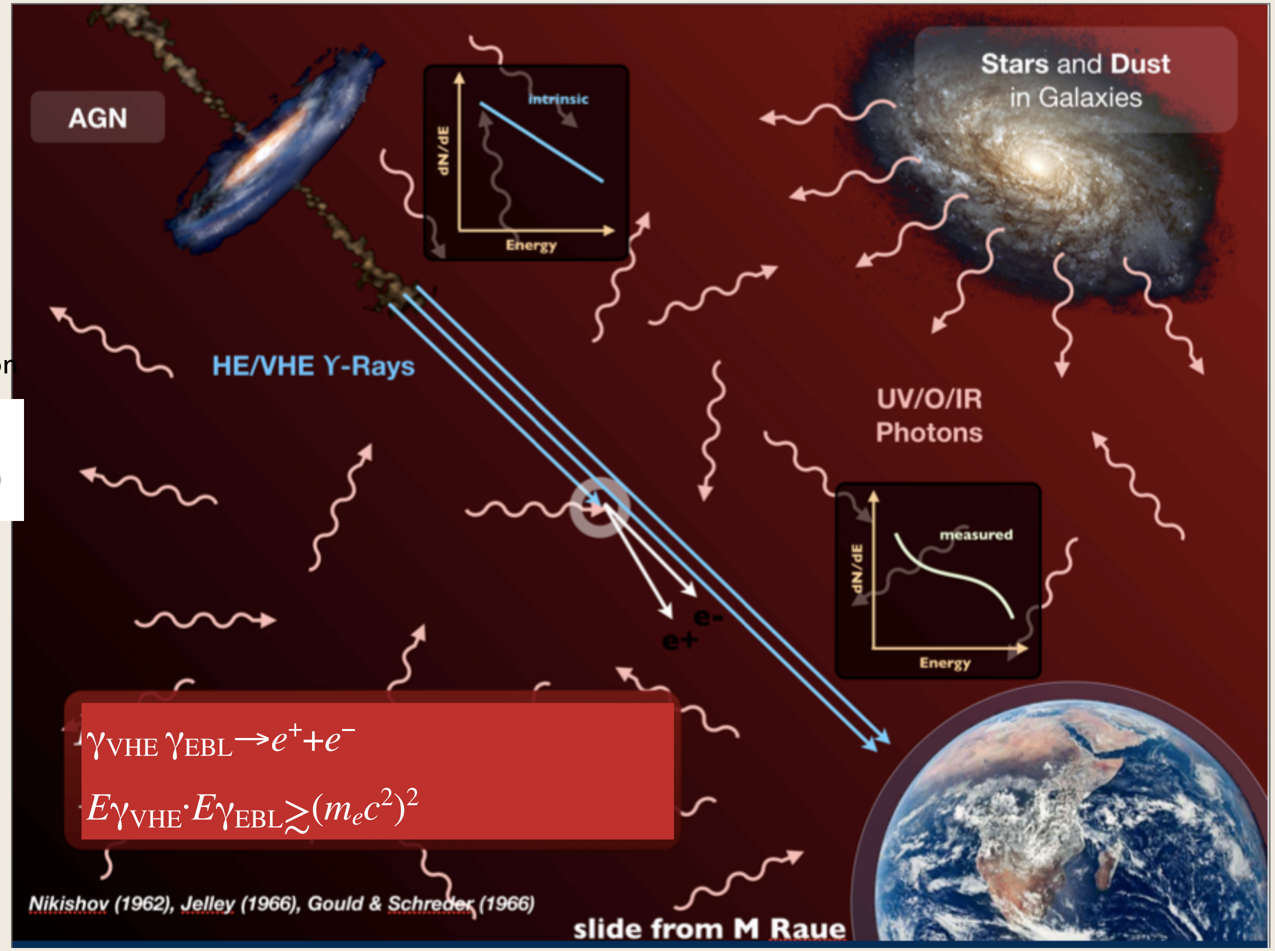

Optical depth = effective absorption of gamma-rays with observed energy E for a source at redshift z:

Space element change with redshift due to Hubble expansion

Proper number density as a function of energy of EBL photon

$$\tau_{\gamma\gamma}(E,z) = \int_0^z \left(\frac{dl}{dz'}\right) dz' \int_0^2 d\mu \frac{\mu}{2} \int_{\varepsilon_{th}}^{\infty} d\varepsilon' \, \sigma_{\gamma\gamma}(\beta') n(\varepsilon', z'),$$

$$\varepsilon_{th} \equiv \frac{2m_e^2c^4}{E'\mu}$$

Cross section of pair production

$$\beta' = \frac{\varepsilon_{th}}{\varepsilon'(1+z')^2}$$

$\mu = (1 - \cos\theta)$, with θ the angle of the interaction

Biteau and Williams 2015
Dominguez et al, ApJ 2019

EBL optical depth evolution with z

Extragalactic source spectrum

$$\left(\frac{\mathrm{d}N}{\mathrm{d}E}\right)_{\mathrm{obs}} = \left(\frac{\mathrm{d}N}{\mathrm{d}E}\right)_{\mathrm{int}} \exp\left[-b \cdot \tau_{\gamma\gamma}\left(E, z\right)\right]$$

D11 (Dominguez 2011, Finke 2010, G12 Gilmore 2012

MAGIC arXiv:1904.00134

b = 0 no attenuation

b=1 attenuation accordng to model

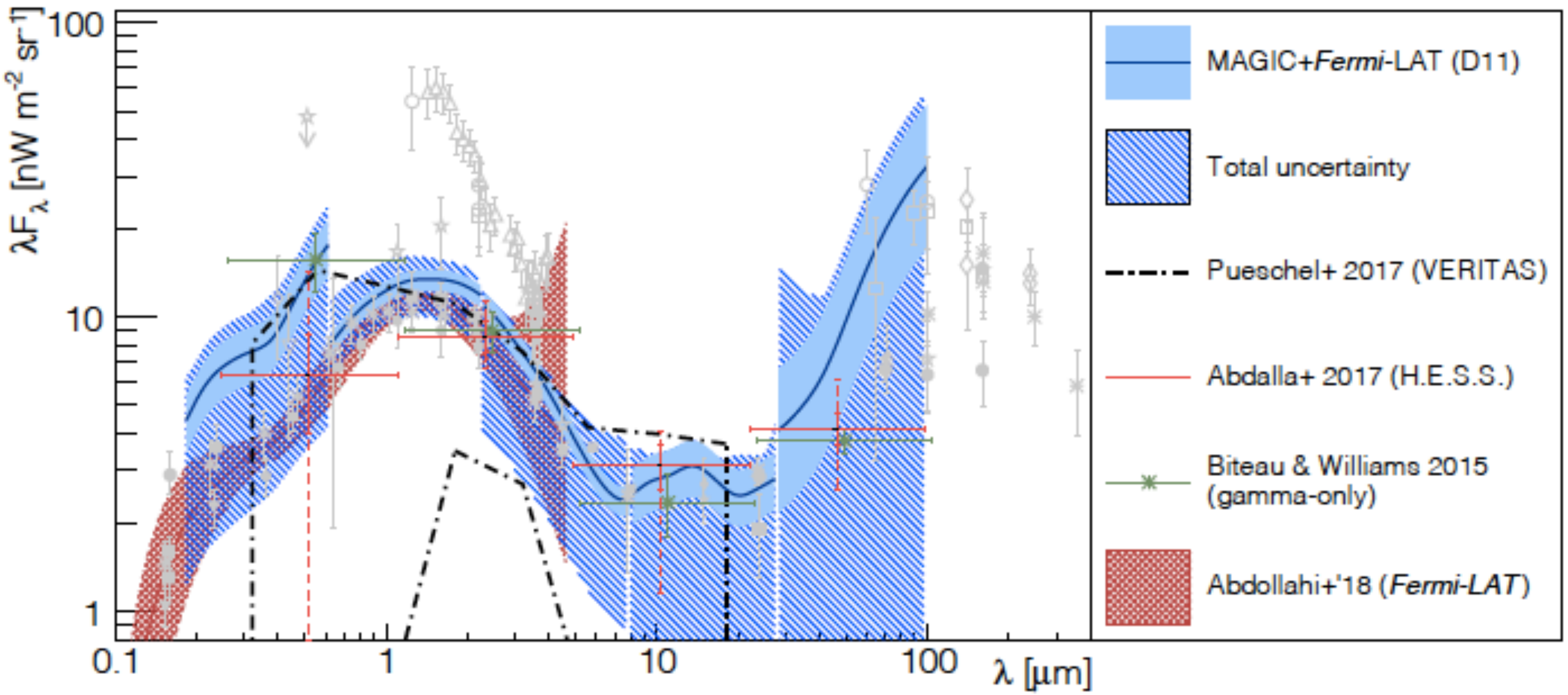

Dominguez et al, ApJ 2019, Grey band: H_0 = 40-95 kms/s/Mpc, $\Omega_m = 0.32$

https://science.sciencemag.org/content/362/6418/1031

Redshift evolution of Extragalactic background light

$H_0 D_L = cz$ from NS-NS merger H0 $=70^{+12}_{-8}$ km/s/Mpc

Abbott et al.,Nature, 24471 (2017)

EBL evolution with z still uncertain, hence two models (D11 & Fi10) with different EBL estimates are used.

From GW measurements: From M. Maggiore's colloquium

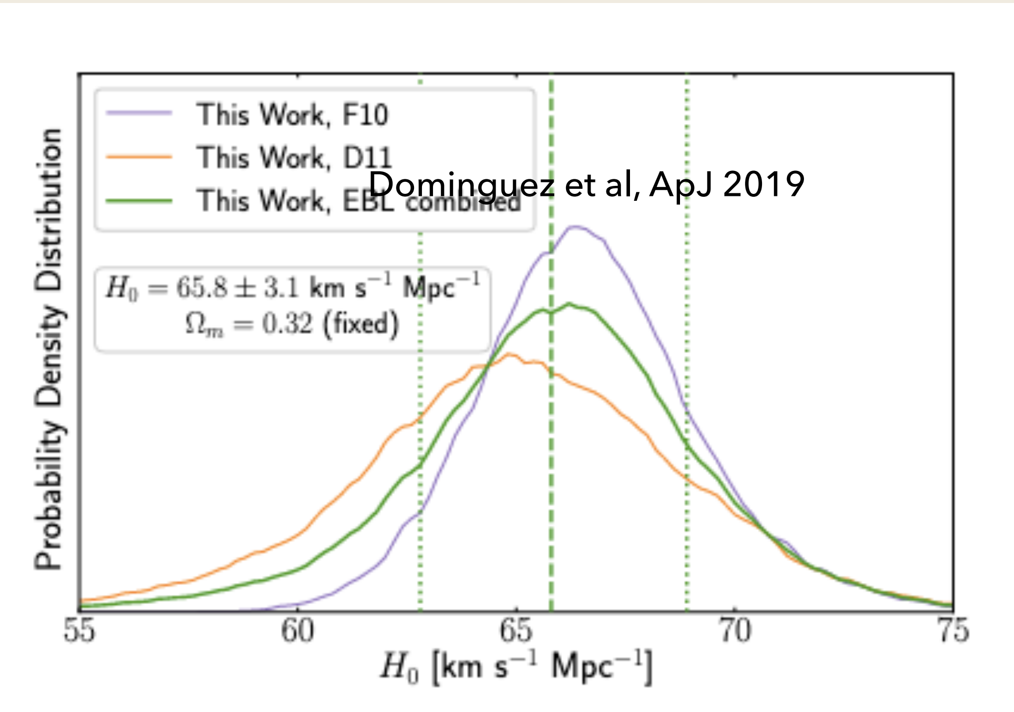

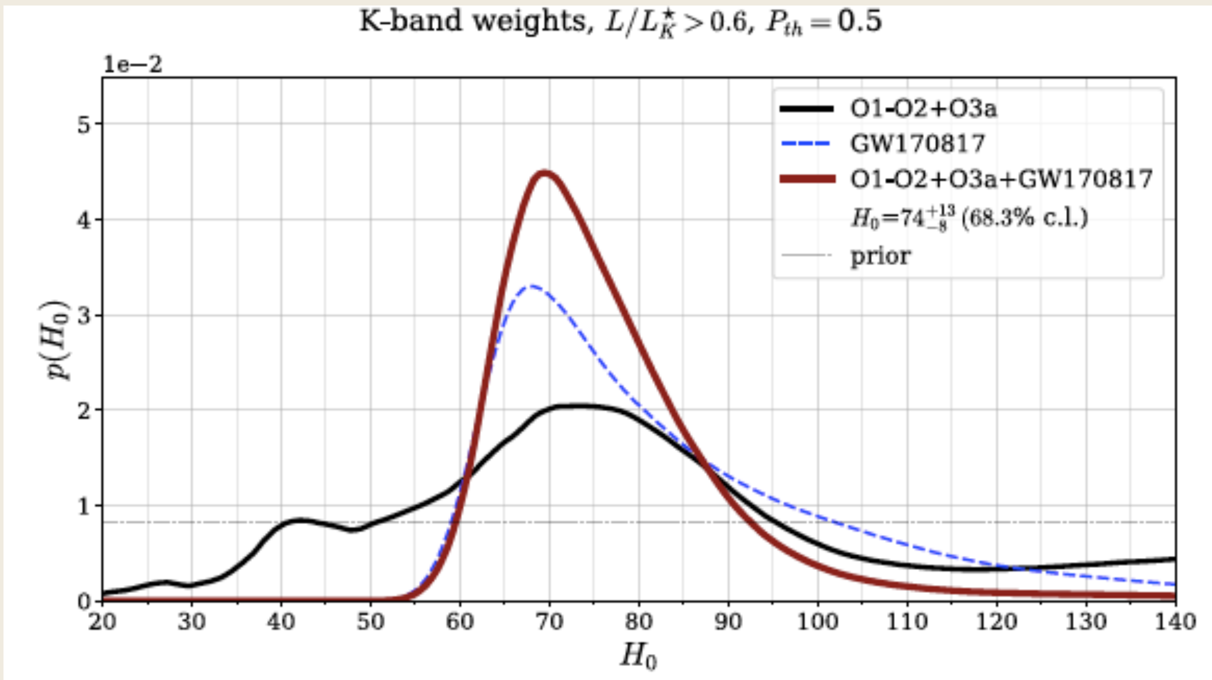

New messenger contributions to H_0 puzzle

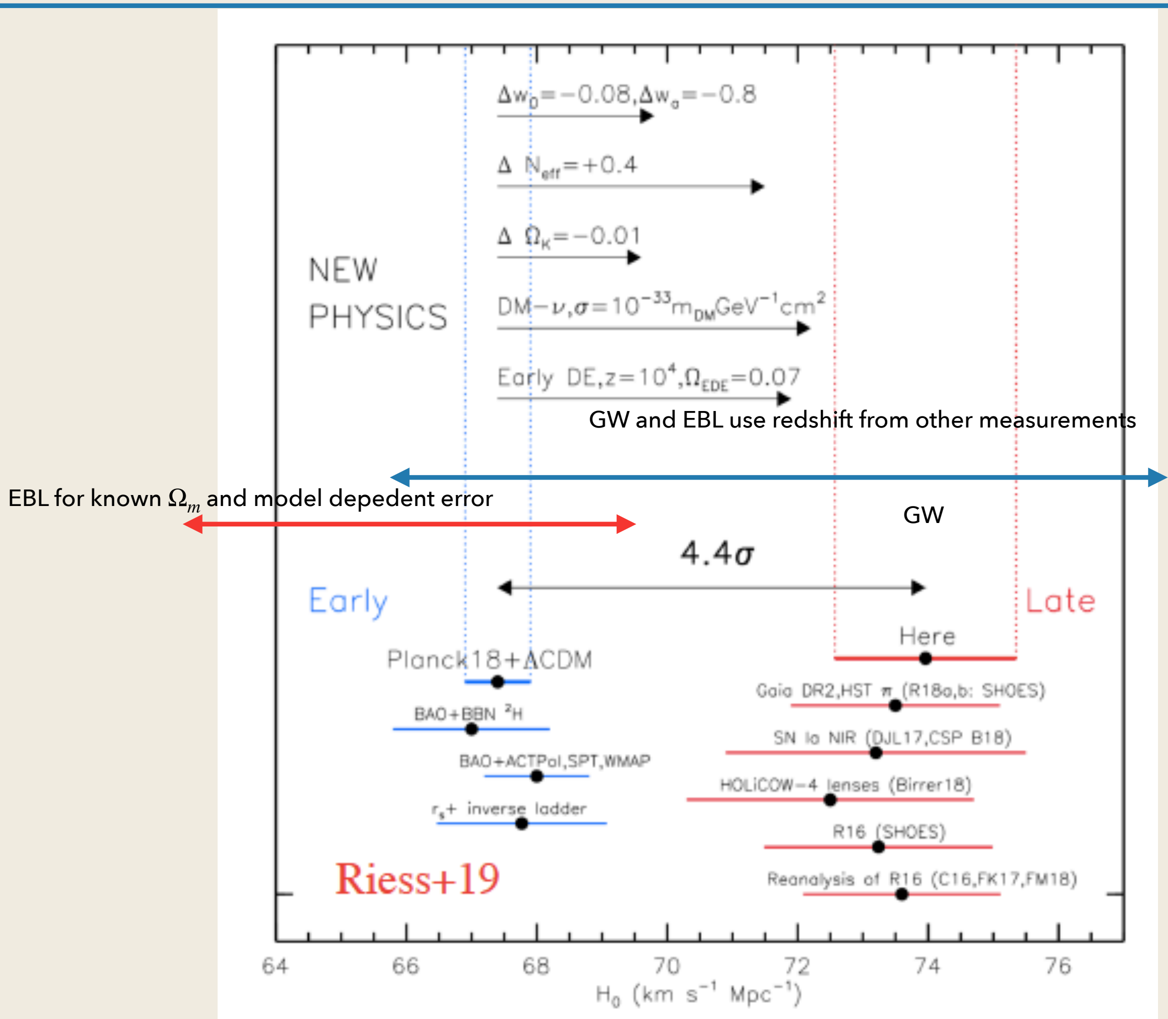

https://arxiv.org/abs/2001.03624

The SST-1M

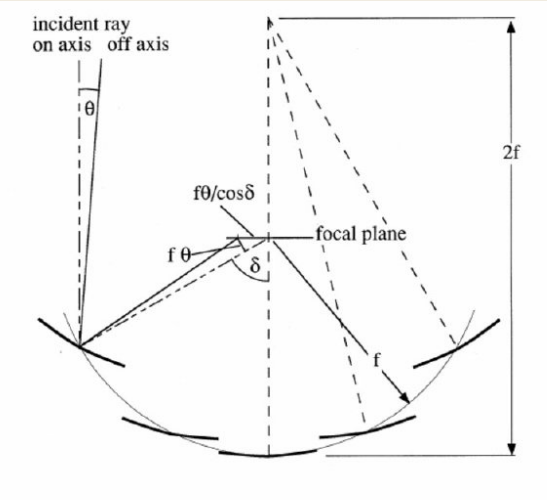

- *Dish = 4 m*
- *FoV = 9°*
- *f/D = 1.4*

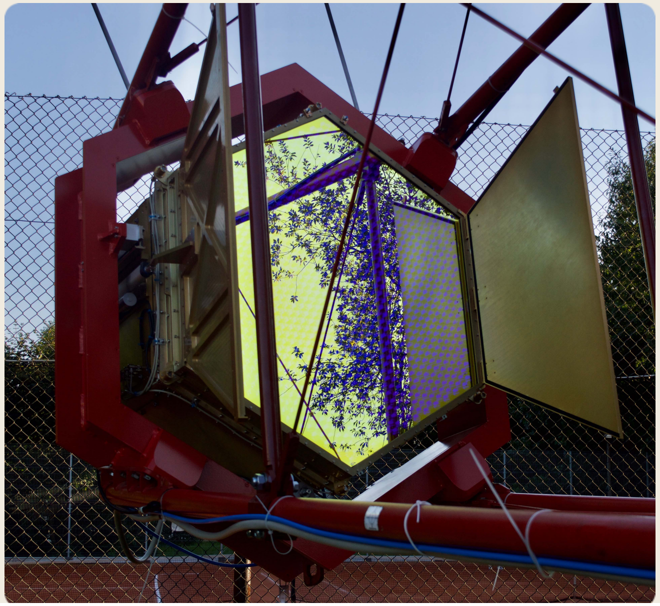

Pixel size = 4· min(σ_x, σ_y) = 0.24°

Camera size ($D_{c)}$) = 88 cm

Pixel size (linear) = 2.32 cm

n_p = 1296 pixels

Watch us on Youtube:
Video 1 (HD) Video 2

SiPM on field

Advantages:

- robustness to light (~30% more observation time)
- Mass producibility, low power, cost

Challenges:

- high sensitivity in night sky background region > 500 nm
- PDE ~10% higher but maximum at too high wavelength for Cherenkov spectrum, need to work at high over-voltage with consequent Xtalk increase and also Voltage drop effect
- Filter on Borofloat improves performance at high energy, at low energy it cuts further than PMMA window in the Cherenkov peak where already SiPM cut more than PMTs

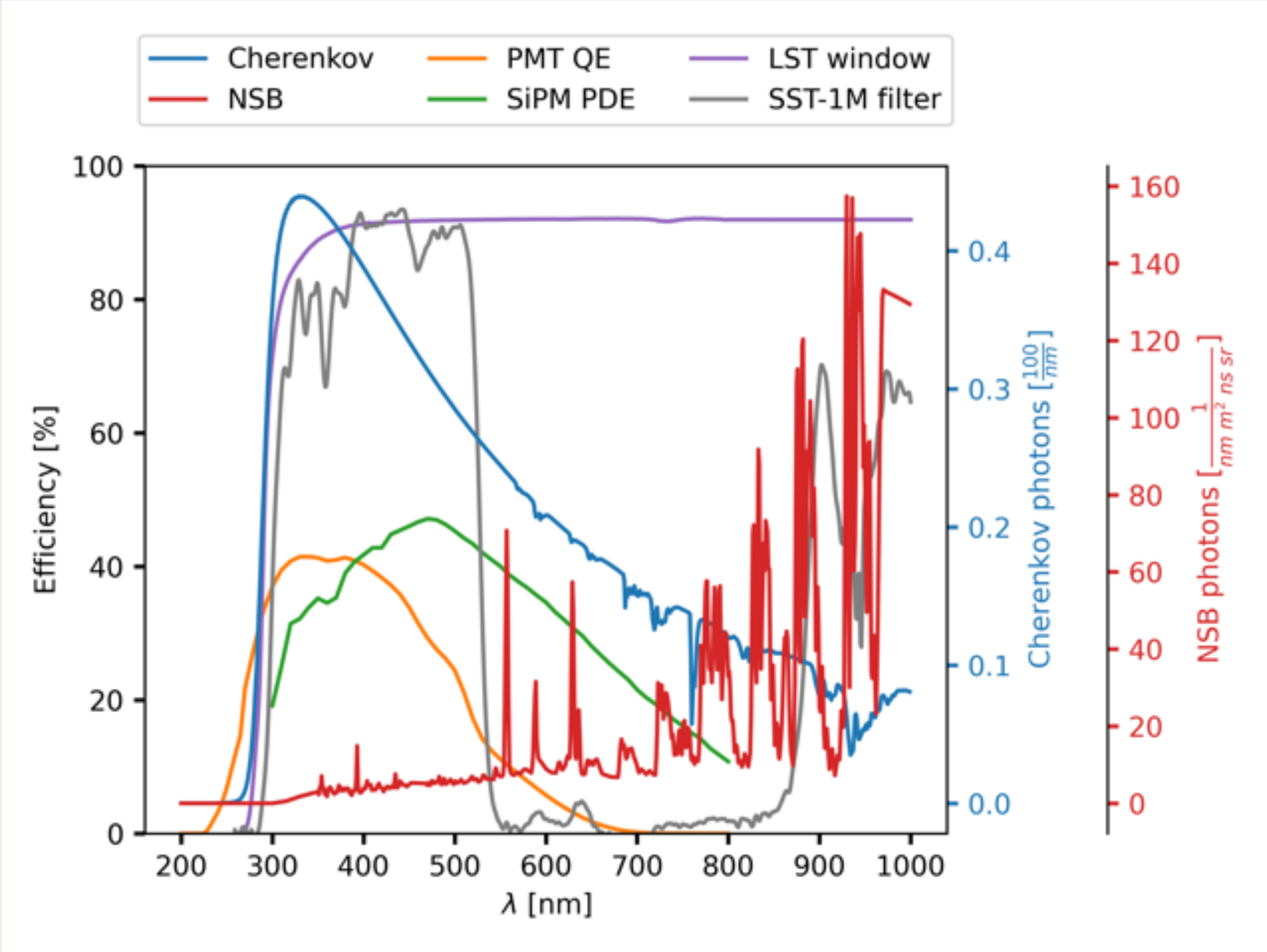

PDE for 8% XTalk

The camera

Hollow light guides:
- Cut-off at 24°
- 2.32 cm linear size
- Compression factor of ~6
- dichroic coating

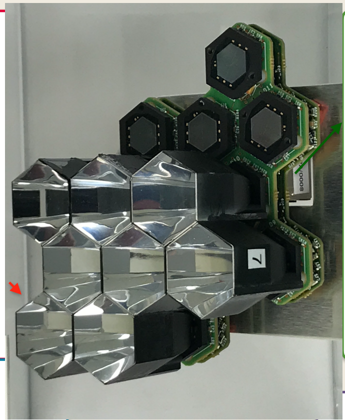

Slow control board:
- 108/camera
- Temperature compensation loop Hz
- HV generation

- 12 bits FADC @ 250 MS/s
- Fully digital trigger, reconfigurable and signal preprocessing
- Serial architecture based on multi-Gigabit links (both trigger and ADC data)
- Power consumption 1200 W

Photo detection plane:
- 1296 pixels
- 0.24° angular size
- Power consumption 500 W
- Analogue signals over CAT5/RJ45

Preamplifier board:
- 108 /camera
- discrete components
- Trans-impedance topology
- DC coupling

- Hamamatsu LCT2 50 um
- 4 anodes per pixel with one common cathode
- NTC temperature sensor

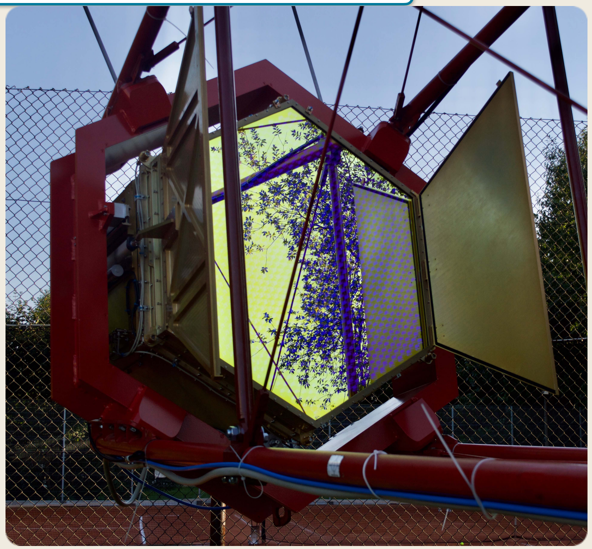

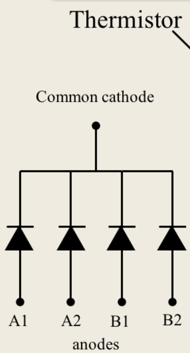

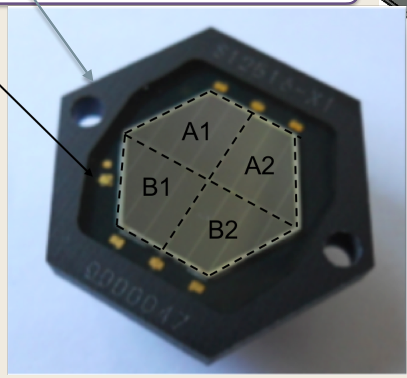

1 cm² sensitive area

$V_{over} = 2.8\ \mathrm{V} \Rightarrow \mathrm{C}_{\mu cell} \sim 85\ \mathrm{nF}$

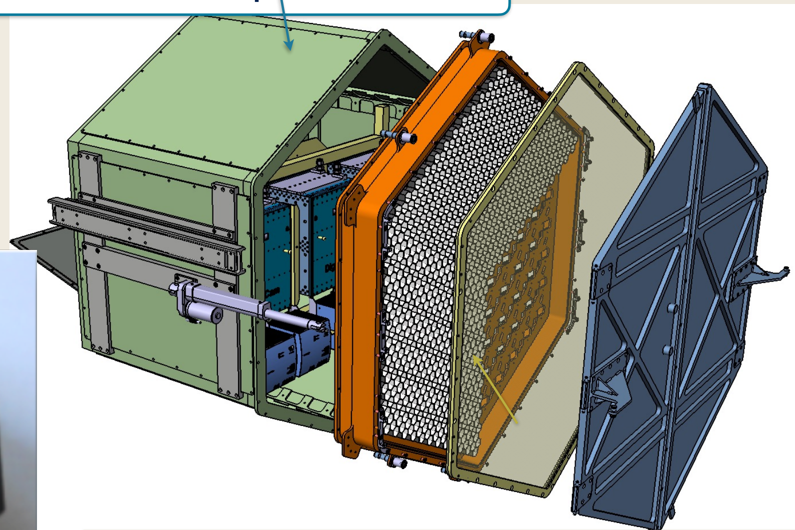

Entrance window:
- 3.3 mm Borofloat
- Cut-off filter at 540 nm for NSB rejection

Heller et al. Eur Phys J C 77 (2017) 1, 47

Events while pointing the Crab (about 2 hrs) with 1 GHz background in Krakow

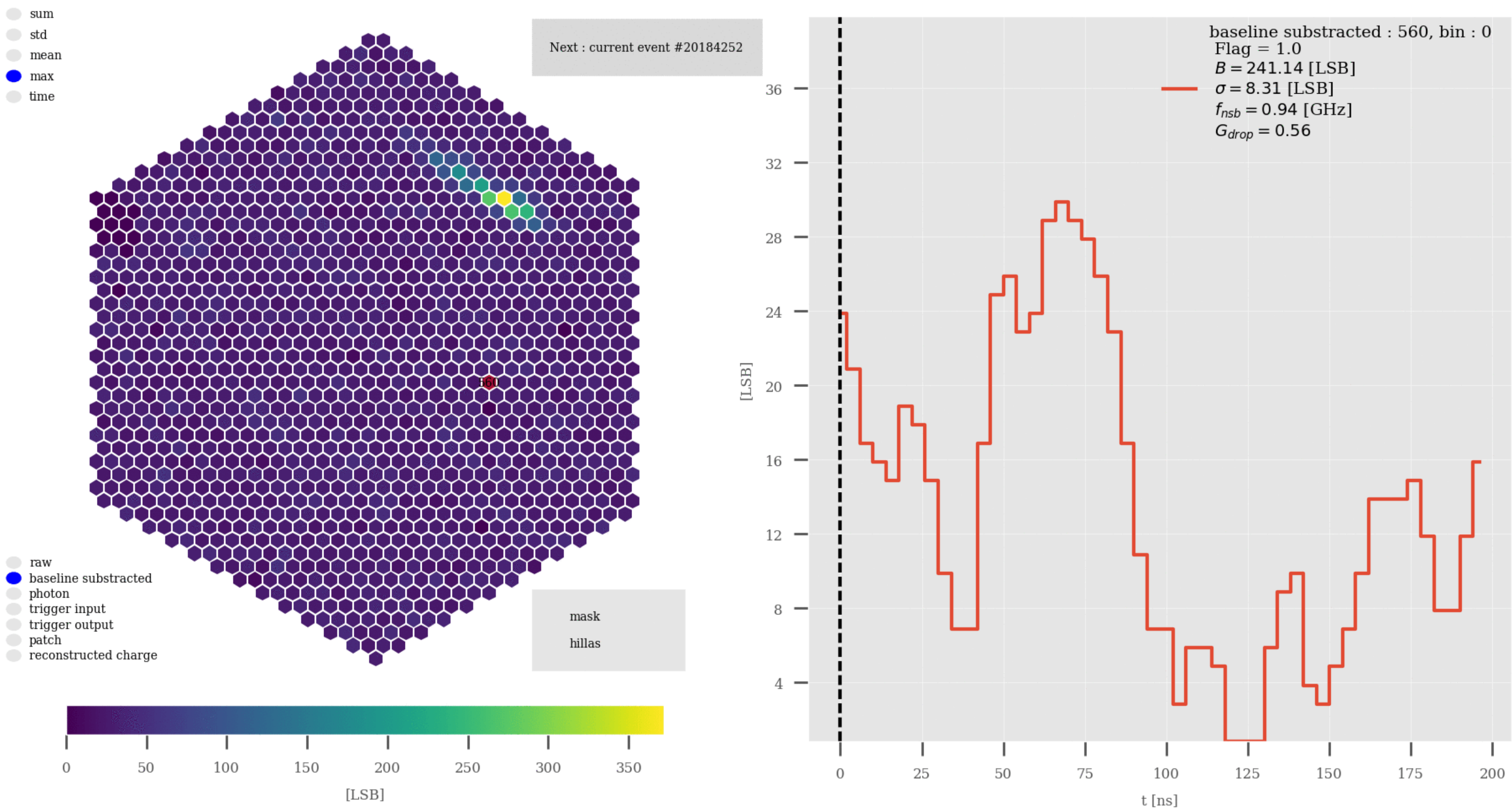

What is Diode?

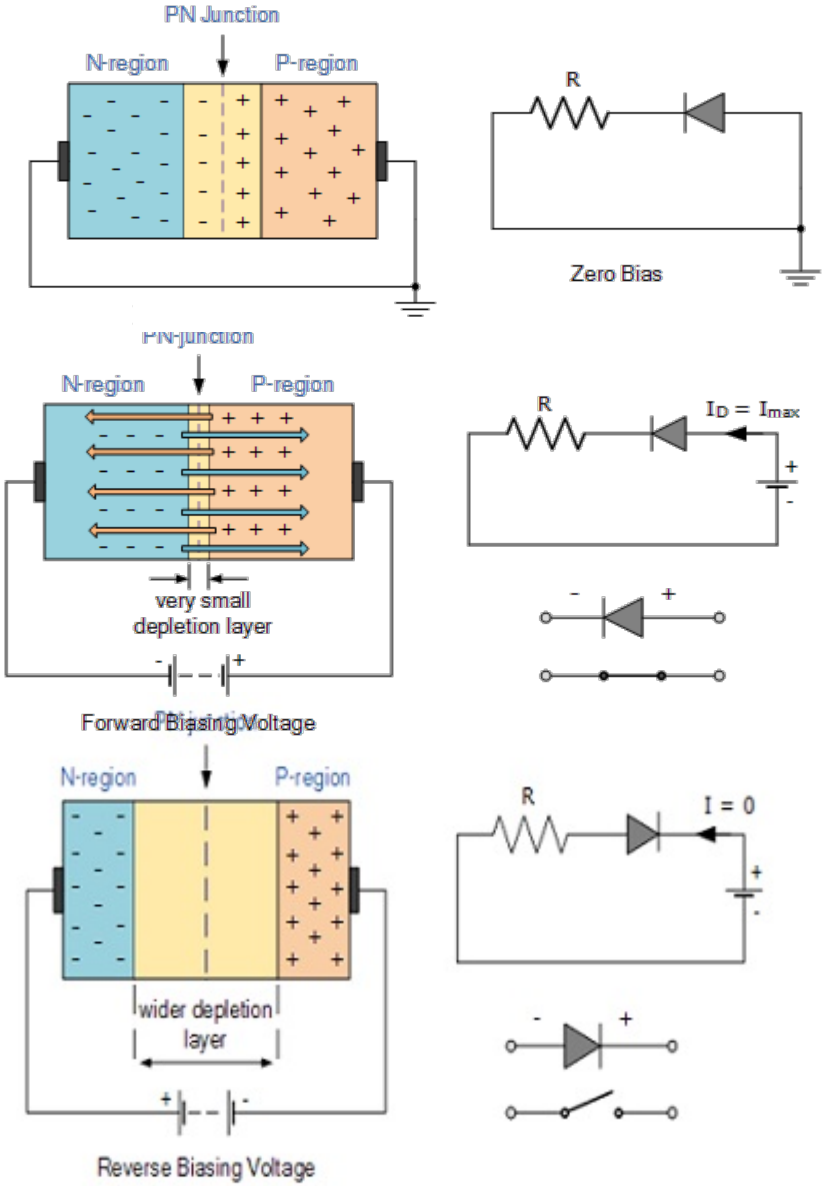

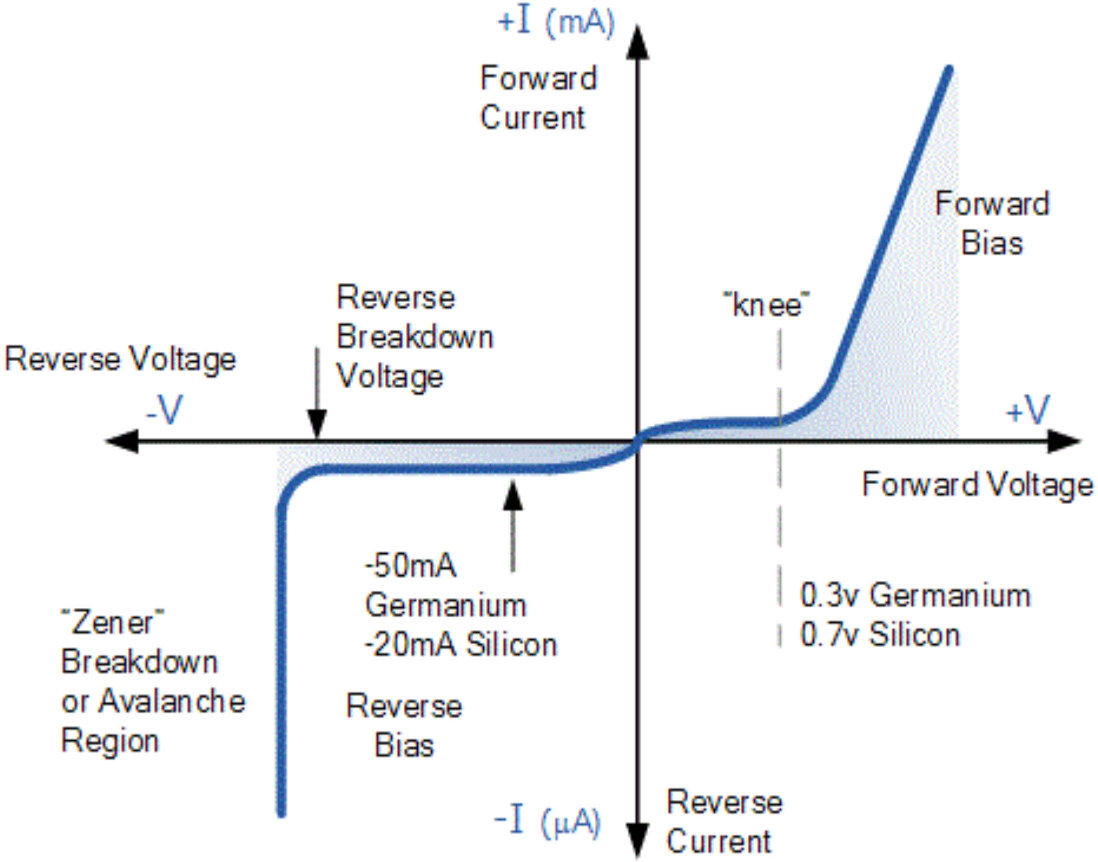

Photon create e-h pare in depleted layer
which can be used to detect light

P-N junction as photon detector

working in reverse bias mode

Current increases exponentially with reverse voltage

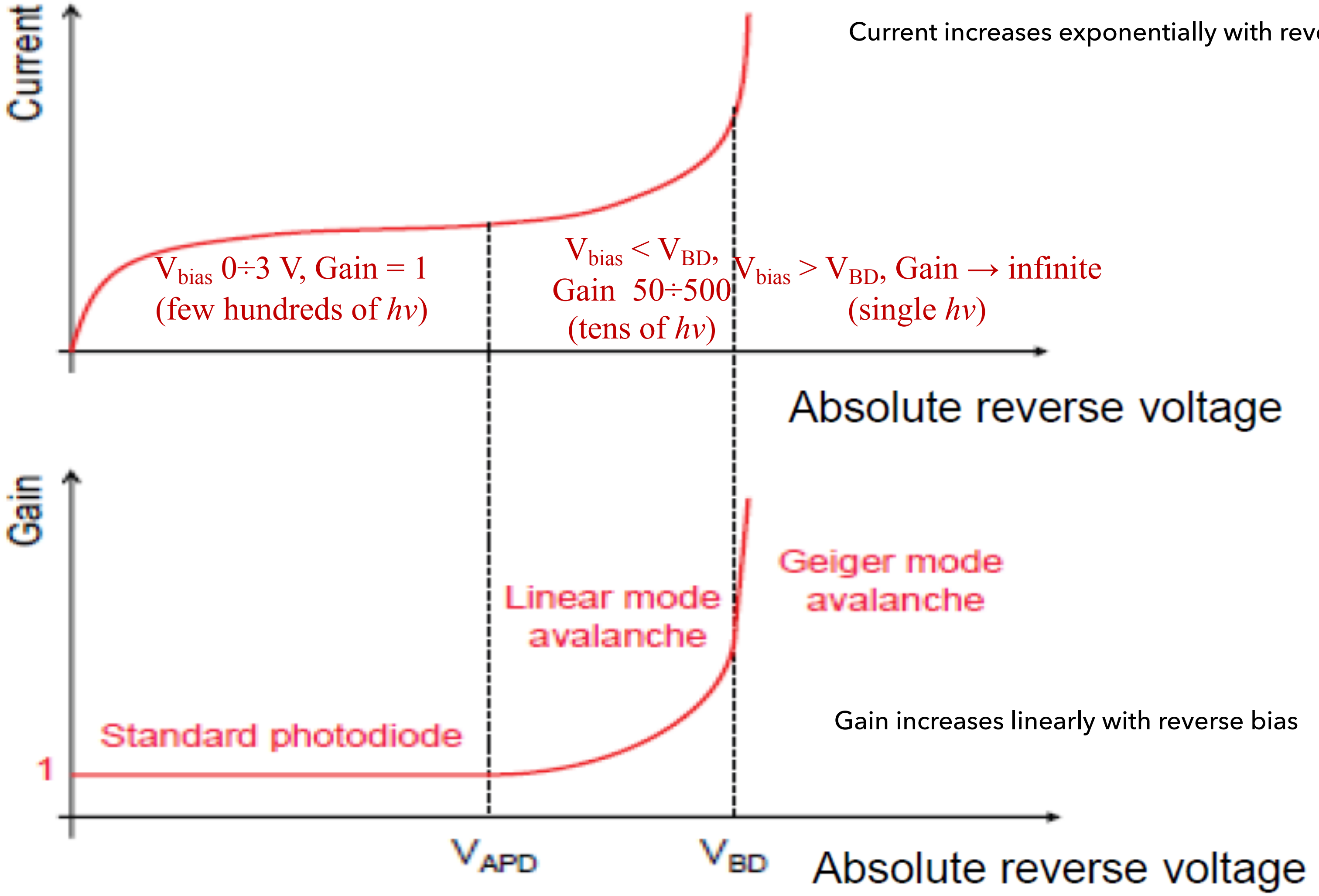

Gain increases linearly with reverse bias

What is SiPM?

Geiger Mode - Avalanche Photodiode

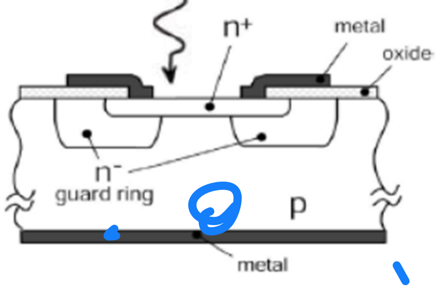

R.H. Haitz, J..A. Phys., Vol. 36, No. 10 (1965)

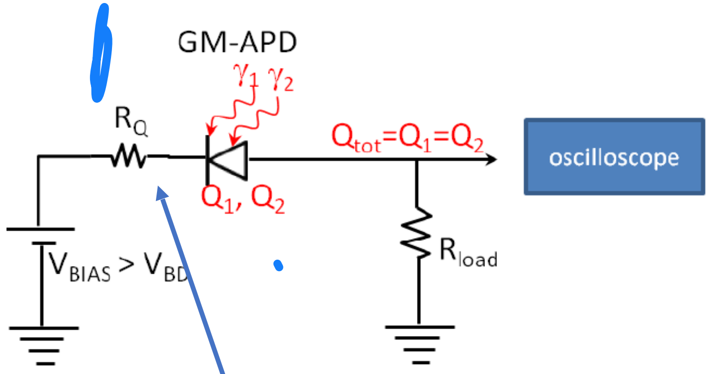

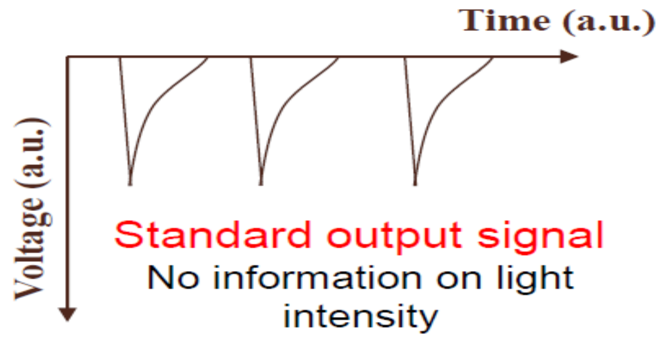

Standard output signal

No information on light intensity

Digital device

$Q = Q_1 = Q_2 = \ldots = Q_n$

Parallel array of μ-cells on the same substrate

- each μ-cell: GM-APD in series with R_q

to quench avalanche

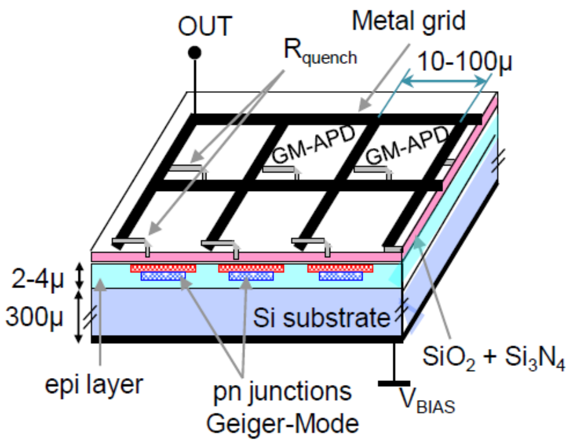

'90s by V.M.Golovin & Z.Sadygov, Russian patents

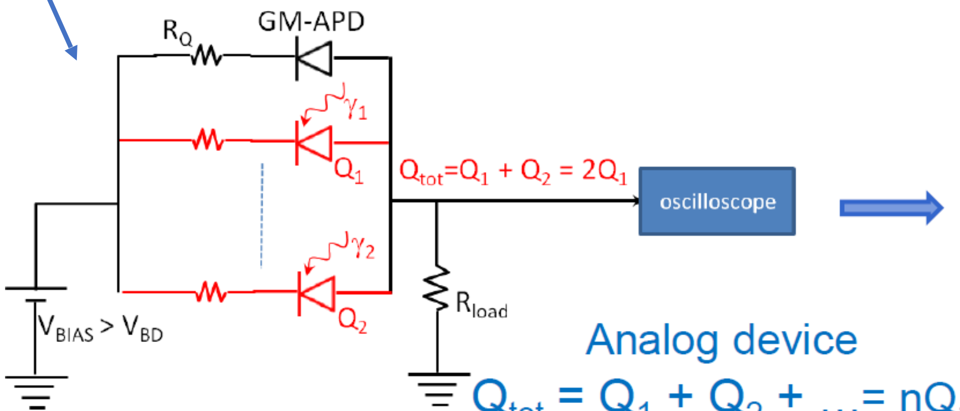

Analog device

$Q_{tot} = Q_1 + Q_2 + \ldots = nQ_1$

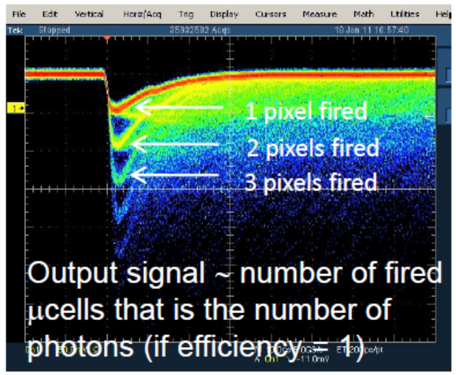

Gain and PDE

Each ucell detects photons identically => the sum of the photocurrents from each ucell combines to form an output providing the magnitude of photon flux. In practice, G is measured from integration of pulse - baseline.

$$G = \frac{Q}{e} = \frac{1}{G_{Amp} \cdot e} \cdot \frac{1}{R} \int (V(t) - BL)\, dt$$

Amplifier input impedance

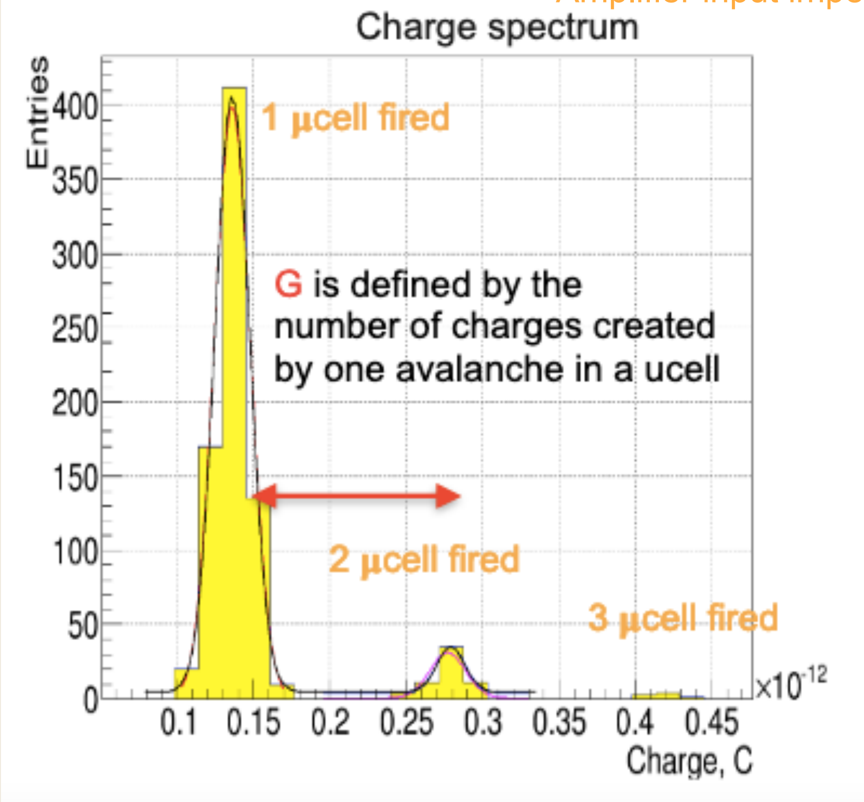

Photon detection efficiency PDE

- $PDE = QE(\lambda, T) \times P_{Geiger} \times FF$

QE – probability to create an e/h pair
P_{Geiger} – probability that e/h triggers an avalanche
FF – ratio between active and total areas

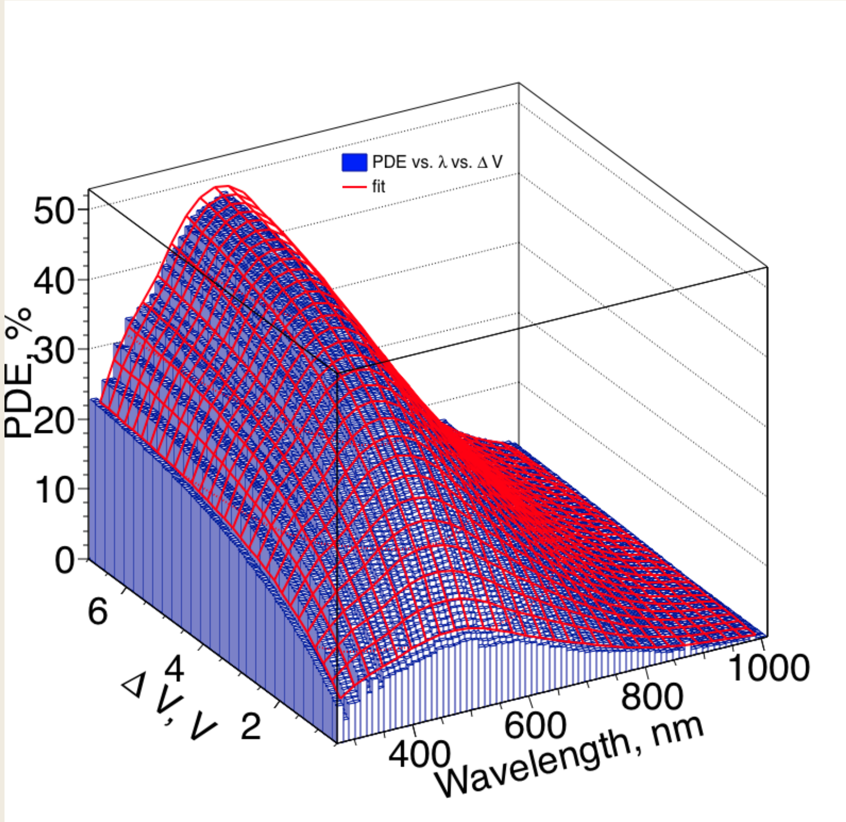

Calibrating SiPMs

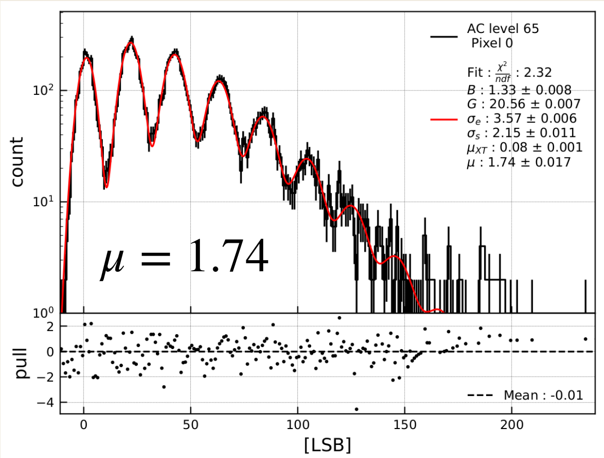

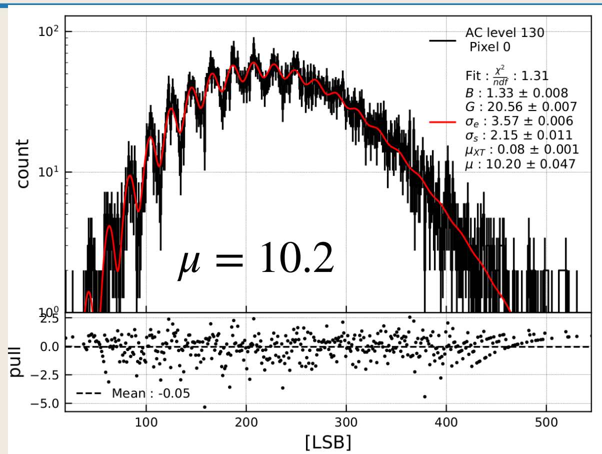

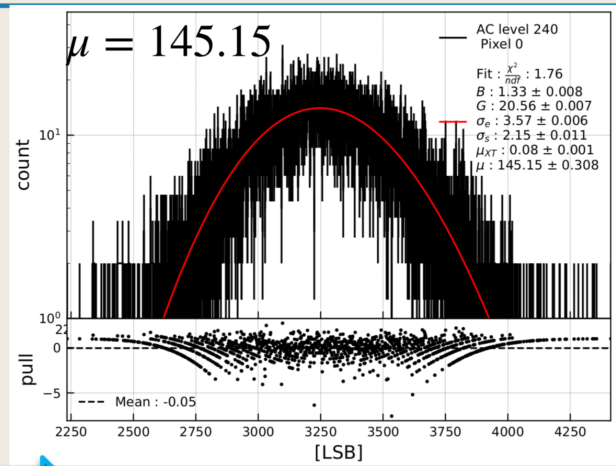

Increasing light level

Smeared generalised Poisson evaluated for each light level *j*:

$$P(C_j = x) = \sum_{k=0}^{\infty} \frac{\mu_j(\mu_j + k\mu_{XT})^{k-1}}{k!} e^{-\mu - k\mu_{XT}} \frac{1}{\sqrt{2\pi}\sigma_k} e^{-\frac{(x-k\bar{G}-\bar{B})^2}{2\sigma_k^2}}$$

With $\sigma_k^2 = f\Delta t\sigma_e^2 + k\bar{G}\sigma_s^2$ Δt: integration window f: sampling frequency

G: charge gain, i.e. pulse integral
B: residual charge
μ_{XT}: Cross talk fraction
σ_e : electronic noise
μ_j: average p.e. number

Maximum log-likelihood estimation per light level and per pixel:

$$l(\vec{\theta}; C_j) = \frac{1}{N_w} \sum_{i=1}^{N_w} \ln \mathcal{L}(\vec{\theta}; C_{ij})$$

($\vec{\theta}$: fit parameters)

All fitting parameters are independent of the light level (LL), aside from μ_j => all light levels are combined for the fitting

$$\hat{l}(\vec{\theta}; C) = \frac{1}{N_w N_{AC}} \sum_{j=1}^{N_{AC}} \sum_{i=1}^{N_w} \ln \mathcal{L}(\vec{\theta}; C_{ij})$$

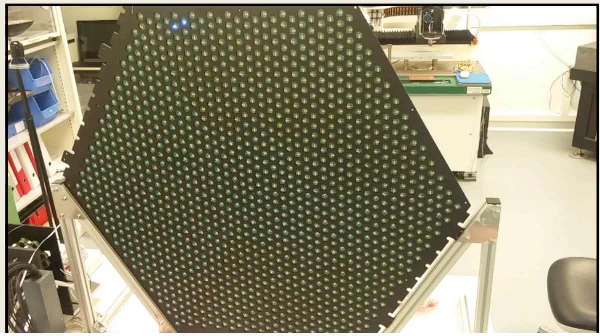

Alispach et al, arXiv:2008.04716, C. Alispach PhD Thesis

Performance measurements

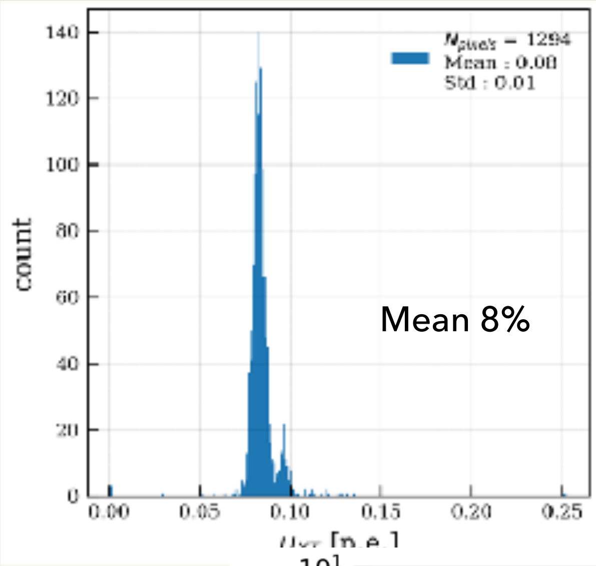

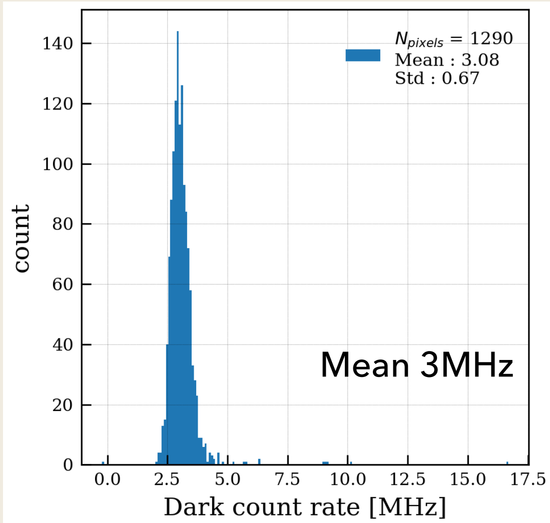

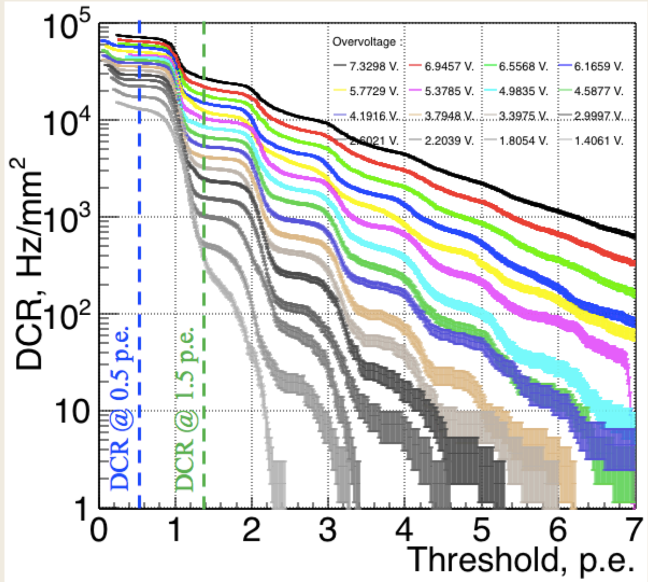

125 MHz/pixel NSB

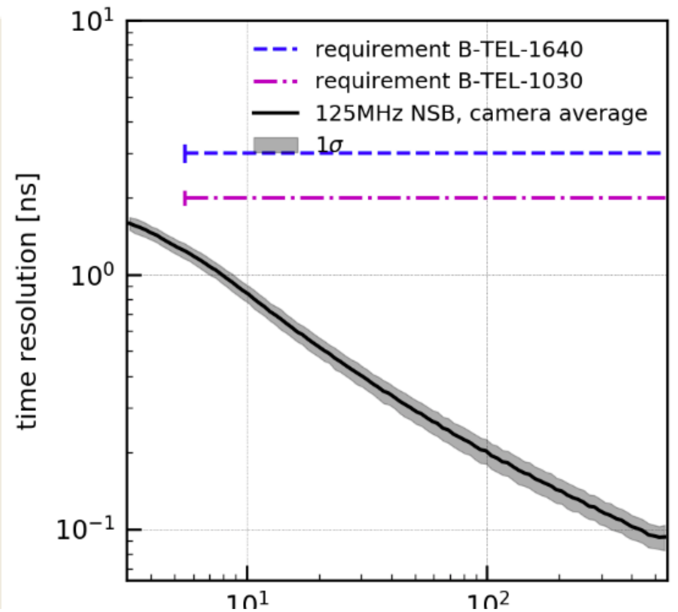

Charge resolution

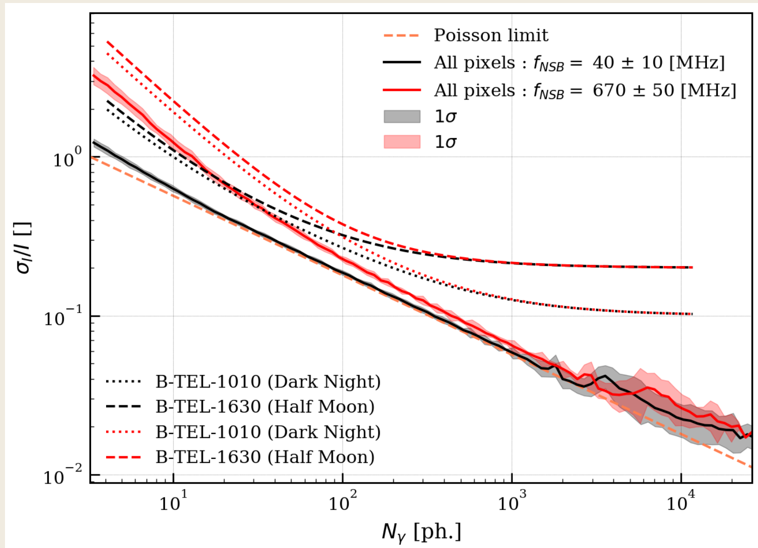

Trade-off of PDE / XT for SiPM @ room temperature and with large light rates

Increasing overvoltage increases PDE and XT. Night Sky Background increases with PDE.

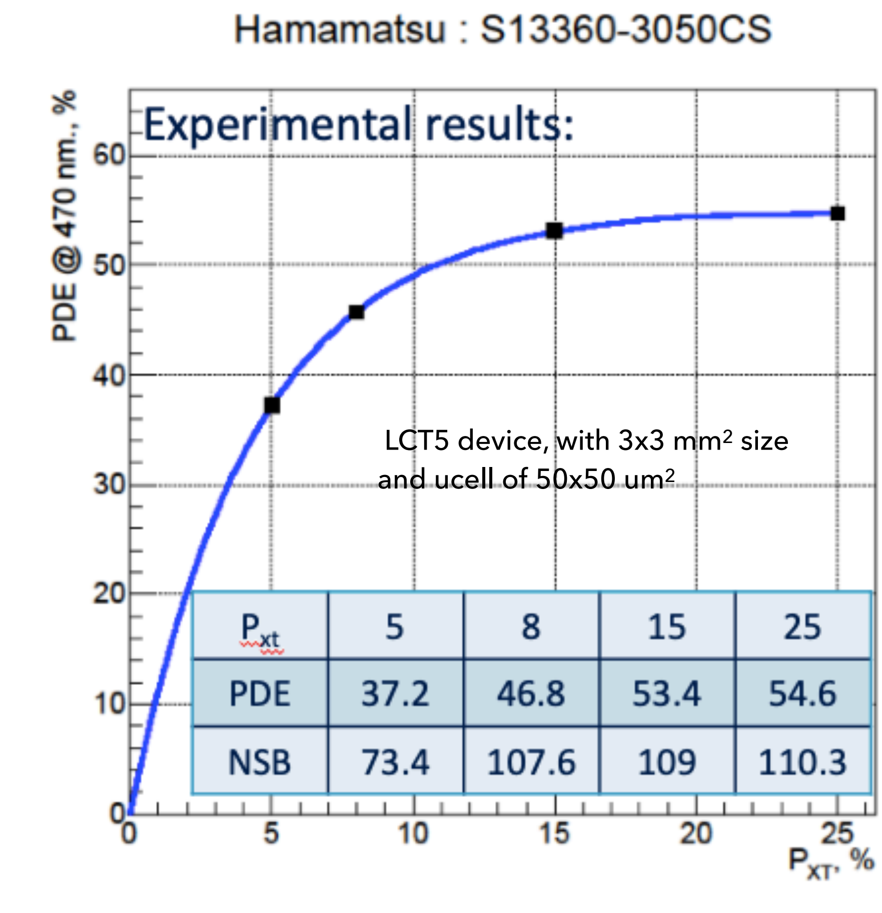

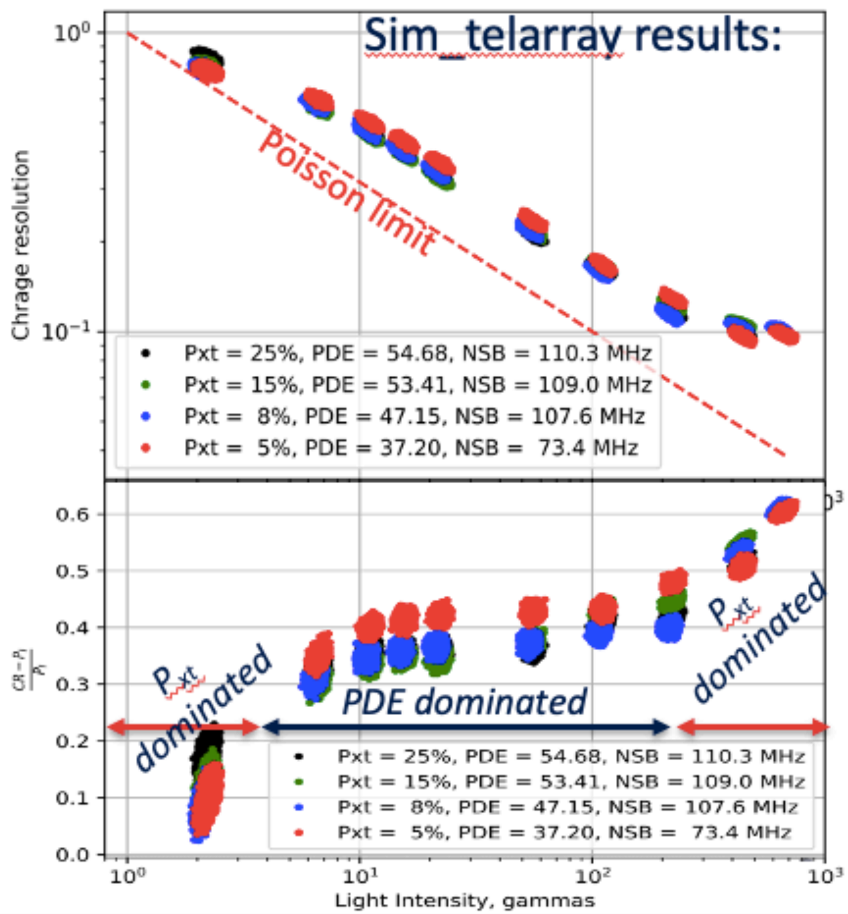

Optical XT : the avalanche process in a ucell emits secondary IR photons that are then detected by the surrounding ucells with a certain probability (P_{XT}).

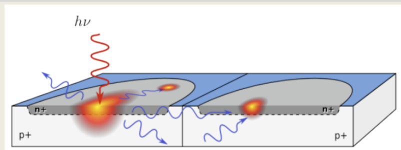

Operation under continuous light

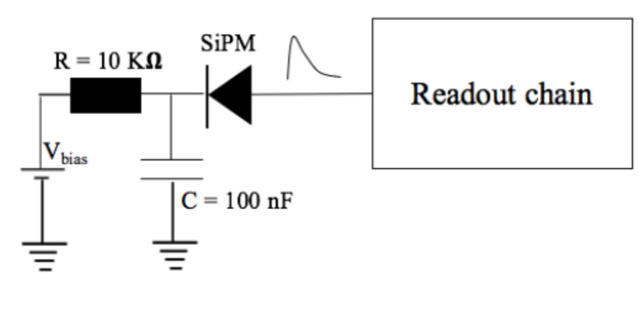

Figure 2: Typical schematics to bias SiPM device.

SiPM devices are usually biased through an RC filter to:
- filter high frequency electronic noise coming from the DC bias source
- limit the current, therefore protect the sensor in case of intense illumination.
- But this resistor also induces a **voltage drop** at the sensor cathode in presence of continuous light, which reduces the bias voltage and therefore changes its operation point

A compensation loop through the slow control board or an offline correction.

http://arxiv.org/pdf/1910.00348.pdf

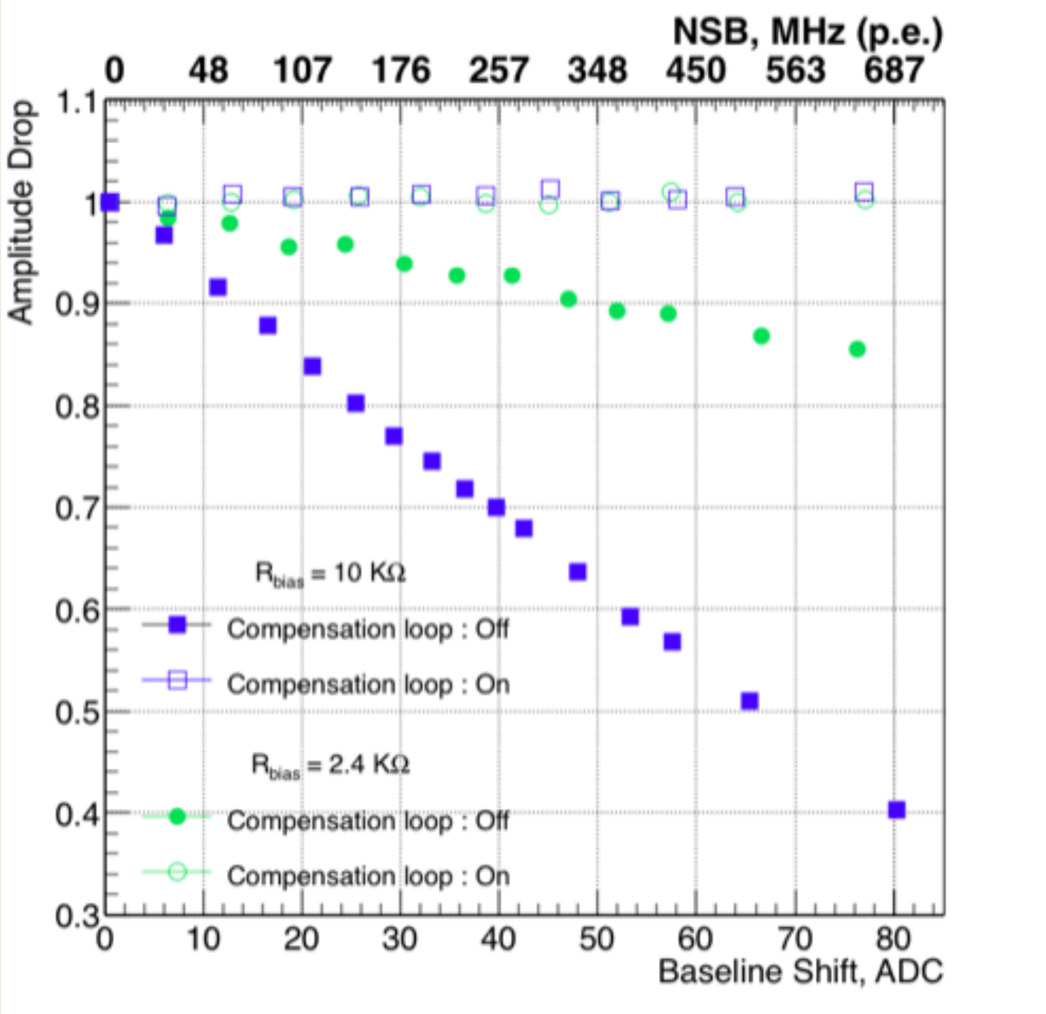

The LST Advanced SiPM Camera

- 4 times more pixels than SST-1M (~8000) => pixel size from 0.1° to 0.05°
    - Increased capabilities of feature extractions for gamma/hadron separation
    - More channels prohibit dual gain;
    - more pixels imply lower amount of light per pixel and so relaxes demands on dynamic range and a single gain can be used;
    - High operation voltage can be used for high PDE since XT effect limited
- Goal: fully digital readout (12 bit FADC @1GSps!)
    - Higher flexibility for:
        - Advanced trigger implementation
        - Data processing inside the camera
        - Updatability/Reprogrammability

But this poses many challenges that require ASICs!

- Power consumption
- Data throughput
- Cost